Functional characterization of the *lpdA* genes in *Sinorhizobium meliloti*

Martina Solano Bielen

Department of Natural Resource Sciences

McGill University

Montreal, Canada

December, 2014

A thesis submitted to McGill University in partial fulfillment of the requirements of the degree of **Master of Science**

Abstract

Sinorhizobium meliloti has three genes with high homology to the *Escherichia coli lpdA* gene. The *E. coli lpdA* gene encodes for the dihydrolipoamide dehydrogenase (LPD) enzyme, the E3 subunit of three multi-enzyme complexes: pyruvate dehydrogenase (PDH), 2-oxoglutarate dehydrogenase (OGD) and a branched-chained α-keto acid dehydrogenase (BKD). In *S. meliloti*, the *lpdA1*, *lpdA2* and *lpdA3* are proximal to the genes encoding for the E1 and E2 subunits of the PDH, OGD and BKD complexes, respectively. The *lpdA1* and *lpdA2* genes are of special interest due to their association with the tricarboxylic acid (TCA) cycle, which generates energy to support symbiotic nitrogen fixation within root nodules of host plants such as *Medicago sativa* (alfalfa). To study these genes further and to determine if the E3 subunits from these complexes are interchangeable, *lpdA1* (Rm30368) and *lpdA2* (Rm30360) mutants were isolated. An *lpdA3* mutant could not be isolated in this study. Rm30368 was unable to grow with succinate as the sole carbon source, while Rm30360 was unable to grow with arabinose as the sole carbon source. Enzyme assays revealed a lack of PDH activity only in extracts of Rm30368, and of OGD activity only in extracts of Rm30360. Moreover, extracts of Rm30368 had 38% less OGD activity than the wild type cells. Alfalfa plants grown on nitrogen-free substrate inoculated with either Rm30368 or Rm30360 were small and chlorotic, with small white pseudonodules, indicative of the failure of the mutants to fix nitrogen. These results indicate that *lpdA1* and *lpdA2* are specific to PDH and OGD, respectively, and that these genes can not substitute the function of each other at native levels of expression.

Résumé

Sinorhizobium meliloti a trois gènes qui ont de grandes similitudes avec le gène *lpdA* de *Escherichia coli.* Le gène *lpdA* de *E. coli* codifie la enzyme dihydrolipoamide déshydrogénase (DLD), la sous-unité E3 de trois complexes multi-enzymatiques; le pyruvate déshydrogénase (PDH), le 2-oxoglutarate déshydrogénase (OGD) et le déshydrogénase des α-keto acides à chaîne ramifiée (BKD). Dans *S. meliloti*, les gènes *lpdA1*, *lpdA2* et *lpdA3* se situent près des gènes qui encodent les sous-unités E1 et E2 des complexes multi-enzymatiques PDH, OGD et BKD, respectivement. Les gènes *lpdA1* et *lpdA2* présentent un intérêt particulier dû à leur association au cycle TCA qui engendre de l'énergie pour soutenir la fixation symbiotique de l'azote à l'intérieur des nodules de racines de plantes comme la *Medicago sativa* (luzerne). Pour pousser nos études sur ces gènes et pour déterminer si les sous-unités E3 de ces complexes sont interchangeables, nous avons isolé des mutants de *lpdA1* (Rm30368) et *lpdA2* (Rm30360). Le mutant Rm30368 était incapable de se multiplier dans un milieu où le succinate était la seule source de carbone, tandis que le mutant Rm30360 était incapable de se multiplier dans un milieu où l'arabinose était la seule source de carbone. Un manque d'activité du PDH s'est révélé seulement dans les essais enzymatiques des extraits du mutant Rm30368, et un manque d'activité du OGD s'est révélé dans ceux du mutant Rm30360. De plus, les extraits du Rm30368 présentaient 38% moins d'activité du OGD que les extraits de bactéries de type sauvage. Les plantes de luzerne qui ont poussé dans un milieu sans azote et inoculées avec le mutant Rm30368 ou le mutant Rm30360 étaient petites et chlorotiques, avec de petits pseudonodules blancs, ce qui nous indiquait l'incapacité des mutants à fixer l'azote durant la symbiose. Ces résultats nous indiquent que *lpdA1* et *lpdA2* sont spécifiques à PDH et à OGD respectivement, et que ces gènes ne peuvent pas substituer leur fonction respective dans des conditions normales d'expression.

Acknowledgments

Firstly, I would especially like to thank my supervisor Dr. Brian Driscoll for all the support and guidance he has given me along the progress of my work, as well as the patience he has had with me. I would also like to thank my lab mates, David Meek and Patricia Göerner, for all their help and good advice given to me during the beginning, the middle and most importantly, the last period of this work. Also, thanks to the Whyte and Faucher labs for giving me an excuse to wander out of my lab, which I have much enjoyed.

I also want to thank my mother for her support on every day of this masters program. This masters was possible thanks to you. Moreover, I want to thank my boyfriend for his encouragement and his patience, especially during the last moments of the elaboration of my thesis. Thanks to you I was able to have possibly the best two before-submission weeks a grad student can wish for.

Thanks to NSERC for the financial support given throughout my masters program.

Table of Contents

List of Abbreviations

ATP	adenosine triphosphate
BKD	branched-chain α-keto acid dehydrogenase complex
Cm	chloramphenicol deoxynucleotide triphosphate
CoA	coenzyme A
dH_2O	distilled water
DNA	deoxyribonucleic acid
EDTA	ethylene diamine tetra-acetic acid
FAD^+	flavin adenine dinucleotide
GCV	glycine cleavage multienzyme system
Fix+/-	positive/negative nitrogen fixation
Gm	gentamycin
IPTG	isopropyl β-D-1-thiogalactopyranoside
k	growth rate constant
Km	kanamycin
LB	Luria-Bertani medium
LBmc	Luria-Bertani medium with added magnesium and calcium
LPD	dihydrolipoamide dehydrogenase
M9	minimal medium 9
MDH	malate dehydrogenase
NAD+	nicotinamide adenine dinucleotide
NADH	reduced nicotinamide adenine dinucleotide

Nm	neomycin
OADHC	oxo-acid dehydrogenase complex
OD_{xxx}	optical density at a wavelength of XXX nanometers
OGD	2-oxoglutarate dehydrogenase
ORF	open reading frame
PCR	polymerase chain reaction
PDH	pyruvate dehydrogenase complex
RNase	ribonuclease
RT	room temperature
SA	specific activity
SD	standard deviation
SE	standard error
SDS	sodium dodecyl sulfate
Sm	streptomycin
Tc	tetracycline
TCA	tricarboxylic acid
TE	tris-EDTA buffer
TPP	thiamine pyrophosphate
WT	wild type
X-gal	5-bromo-4-chloro-3-indolyl-β-D-galactopyranoside

List of Figures

List of Tables

1 Literature Review

1.1 Rhizobia provide biological nitrogen fixation

Rhizobia include a broad range of soil bacteria mainly from the α-proteobacteria class. All rhizobia can establish a symbiotic relationship with legume plants. The interaction between bacteria and plant is established within root nodules. Martinus Beijerinck, a Dutch microbiologist found out these nodules contained microbes, which he designated as rhizobia (Chung and Ferris, 1996). The nodules supply the rhizobia with a favourable environment as well as carbon and energy sources. In return the bacterial endosymbionts, called bacteroids, convert atmospheric nitrogen into ammonia-nitrogen for the plant in a process called biological nitrogen fixation (Dymov et al., 2004; Galibert et al., 2013). Since their discovery and isolation, rhizobia have been used instead of commercial nitrogen fertilizers for leguminous plants (Pauu, 1991). Rhizobia also have become a restless focus of research, especially in the understanding of the plant-microbe relationship.

Many rhizobia species have been isolated and been classified in genera, including *Sinorhizobium*, *Mesorhizobium*, and *Bradyrhizobium.* Each species associates with a narrow range of plants of the same genus, triggering the formation of nodules. The specificity between species is determined by the nodulation factors released by the bacteria and the flavonoids produced by the legumes released into the rhizosphere (Peters et al., 1986).

Once the bacteria reach the inside of the plant cells, they irreversibly differentiate into bacteroids and become genetically re-programmed. Genes for nitrogen fixation (*nif* genes) and associated processes (*fix* genes) are induced, and other pathways involved in the cell growth and division are down-regulated (Udvardi et al., 2013). Moreover, genes for dicarboxylic acid

catabolism become strongly expressed in bacteroids (Udvardi et al., 2013). The bacteroids become nitrogen fixing factories, fueled by the dicarboxilic acids supplied by the plant cell.

1.2 The tricarboxylic acid cycle provides the energy for biological N fixation

The tricarboxylic acid (TCA) cycle is an essential carbon metabolic pathway for all aerobic organisms that oxidize carbon compounds, including rhizobia. This cycle supplies high amounts of energy in the form of ATP, reducing power, and intermediates that will serve as substrates for many other metabolic and biosynthetic pathways. This cycle has been intensively studied in *Escherichia coli* and *Bacillus subtilis*. In rhizobia many details of its components and regulation are still lacking; however, some general features from other prokaryotes can be applied (Dunn, 1998).

Enzyme activity data of the TCA cycle enzymes indicate the presence of a complete TCA cycle in bacteroids (Dunn, 1998). Due to the nitrogenase oxygen lability, the amount of oxygen present in the bacteroids is very low (3 to 22 nM), favouring poor efficiency of this cycle. Despite the suboptimal oxygen levels, the TCA cycle plays a major role in the oxidation of carbon sources and the energy production in rhizobia (Lodwig and Poole, 2003). Nitrogen fixation is a high energy demanding process (16 ATP and 8 reducing equivalents per mol of ammonia produced) that depends largely on the correct working of TCA cycle, as demonstrated by the variety of enzyme mutants (Dymov et al., 2004; Mortimer et al., 1999; Walshaw et al., 1997; McDermott and Kahn, 1992; Gardiol et al., 1982). Plants inoculated with TCA enzyme deficient bacteria were chlorotic and stunted, with N-content values similar to those of uninoculated plants.

The TCA cycle is divided into two sections depending on the nature of the metabolites (Figure 1). The first section is composed of three reactions that use tricarboxylic acids as substrates. Citrate synthase catalyses the irreversible condensation of oxaloacetate and acetyl-CoA to produce citrate. In the next step, the citrate can be reversibly isomerized to isocitrate by the enzyme aconitase. The isocitrate is then oxydized by isocytrate dehydrogenase, yielding the dicarboxilic acid, 2-oxoglutarate (Lodwig and Poole, 2003).

In the second section of the cycle, dicarboxylic acids constitute the substrates of the reactions. The 2-oxoglutarate dehydrogenase catalyses an oxydative decarboxylation of 2-oxoglutarate, yielding a succinyl group linked to a CoA (coenzyme A) cofactor. The succynil-CoA, highly energetic, produces an ATP when converted to succinate by succinyl synthetase. Succinate dehydrogenase oxidizes the succinate to fumarate, which can be reversibly isomerized to malate. Finally, the malate with the help of malate dehydrogenase loses a molecule of water and becomes oxaloacetate, which will be later condensed with a acetyl-CoA molecule (Lodwig and Poole, 2003).

The energy sources provided by the plants to the bacteroids are C_4 dicarboxylic acids such as malate, fumarate and succinate, which are three of the TCA cycle intermediates. Metabolism with C_4 dicarboxylates as sole carbon sources through the TCA cycle is dependant on the input of acetyl-CoA. This metabolism is achieved by the coupled reactions of the malic enzyme (converts malate to pyruvate) and the pyruvate dehydrogenase complex (converts pyruvate to acetyl-CoA; Lodwig and Poole, 2003).

Rhizobia are adapted to free-living styles as well as endosymbiontic lifestyles. Consequently, the proportion of genes dedicated to carbon catabolism and substrate transport is

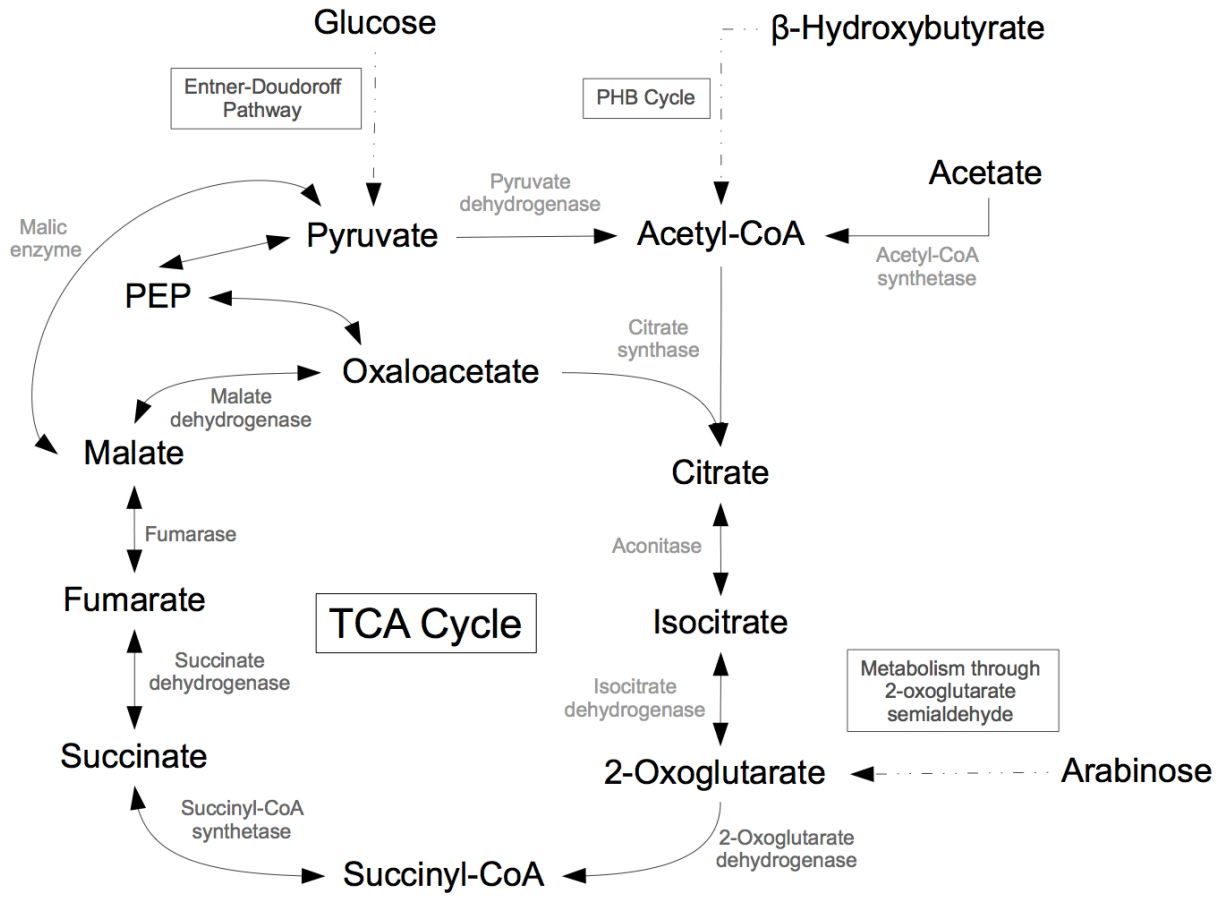

Figure 1: Graphic representation of the tricarboxylic acid (TCA) cycle in *Sinorhizobium meliloti* and examples of pathways which produce TCA cycle intermediates (adapted from Dunn, 1998).

very high compared to other organisms (Galibert et al., 2001). The metabolism of rhizobia differs from some already established model organisms such as *E. coli* and *B. subtilis*; in *Sinorhizobium meliloti* for example, arabinose enters into the central metabolism through the TCA cycle instead of the pentose phosphate and glycolytic pathways as in *E. coli* (Geddes and Oresnik, 2014; Duncan and Fraenkel, 1979).

1.3 *S. meliloti* is a model organism

S. meliloti is the rhizobia species responsible for nodules in legumes of the genera *Medicago* (e.g. alfalfa), *Melilotus* (e.g. sweetclover), and *Trigonella* (e.g. fenugreek). *S. meliloti* is a fast-growing rhizobia. When cultured in yeast extract-mannitol media (YEM), it has generation times of 2 to 4 hours. Slow-growing *Bradyrhizobium* species, which include some of the rhizobia associated to economically important crops such as the soybean and cowpea, have generation times of 6 hours and longer (Sadowsky et al., 1983).

S. meliloti strain 1021, was selected as a streptomycin-resistant derivative of the natural isolate *S. meliloti* SU47 (Krol and Becker, 2004). Strain 1021 was one of the first rhizobial strains for which genome and megaplasmids were completely sequenced (Capela et al., 2001; Galibert et al., 2001). This strain has a well-developed selection of genetic and molecular techniques, such as conjugation, transduction, as well as suitable cloning systems. Many scientists have studied this symbiont, resulting in a large database of genes and mutant strains with exclusive and useful properties. Other interests in *S. meliloti* lie in its nature as an α-proteobacteria, which relates it to some plant and animal pathogens such as *Agrobacterium* and *Brucella* (Galibert et al., 2013).

Much of the genetic and molecular aspects of N_2-symbiosis have been discovered by the study of the systems *S. meliloti-M. sativa* or *S. meliloti-M. truncatula* (Sulieman et al., 2013). Both of these *Medicago* plants are easy to manipulate and grow quickly. *M. sativa* (alfalfa) is one of the most important forage crops in the world, with the potential to increase nitrogen fertility for subsequent crops in a rotation without fertilization (Li and Brummer, 2013). On the other side, *M. truncatula* (barrel medic), closely related to alfalfa, has emerged as a plant model for legumes, due to its small diploid genome, its reproduction properties and the availability of its genomic sequence, among others (Sulieman et al., 2013). Thus, *S. meliloti* is a model organism for rhizobia, because of its relationships with its host *Medicago* legumes as well as its inherent properties and the previous research on it.

1.4 2-Oxo acid dehydrogenase complexes in *S. meliloti*

2-Oxo acid dehydrogenase complexes (OADHCs) are large multi-enzyme complexes that catalyze the conversion of 2-oxo acids to acyl-CoA derivatives. These complexes consist of multiple copies of three types of enzymes: a thiamin diphosphate (TPP)-dependent 2-oxoacid decarboxylase (E1), a dihydrolipoamide acyltranferase (E2) and a NAD^+ dependent dihydrolipoamide dehydrogenase (E3) (Figure 2; de Kok et al., 1998; Payne et al., 2010). In gram-negative bacteria, such as rhizobia, the core of the complex is formed by 24 copies of the E2 component in octahedral symmetry. A lipoic acid is covalently bound to the E2 subunit by an amide bond (lipoamide). This involves the carboxyl group of the lipoic acid and the amino group of a lysine residue from a conserved amino acid sequence of the E2 subunit (Ambrose and Perham, 1975; Cabanes et al., 2000). The end of the lipoic acid contains a dithiolane ring that

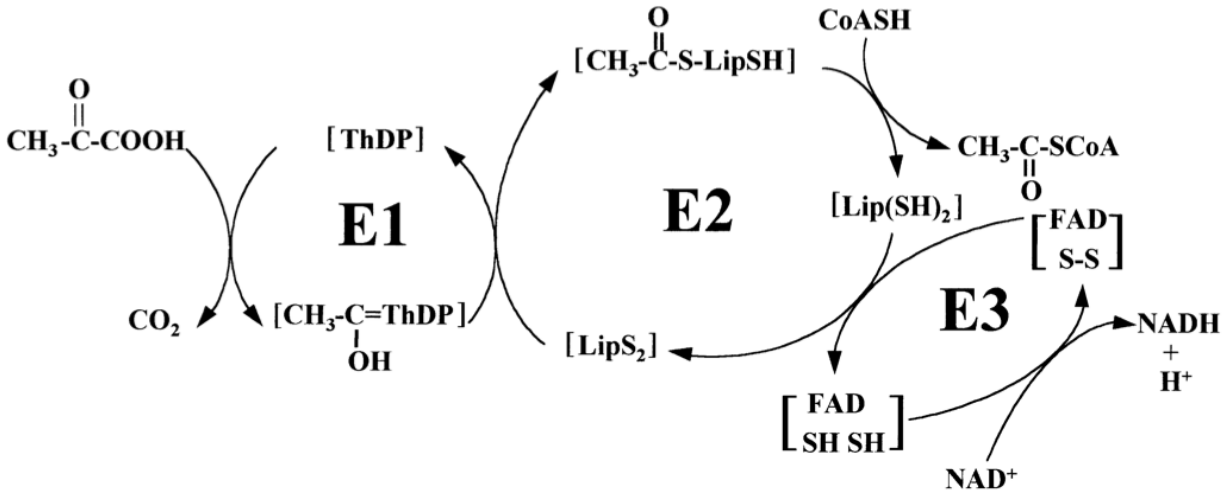

Figure 2: Graphic representation of the mechanism by which the pyruvate dehydrogenase complex converts pyruvate to acetyl-CoA (de Kok et al., 1998). E1, E2 and E3 represent the different types of subunits.

connects the three active sites and channel the substrate through the complex.

There are three OADHCs in the TCA cycle: the pyruvate dehydrogenase complex (PDH),the 2-oxoglutarate dehydrogenase complex (OGD) and the branched-chain α-keto acid dehydrogenase complex (BKD).

1.4.1 Pyruvate dehydrogenase complex (PDH)

PDH catalyzes the oxidative decarboxylation of pyruvate to form acetyl-CoA, linking the glycolysis with the citric acid cycle. In bacteria, these complexes are regulated by product inhibition and allosteric mechanisms (de Kok et al., 1998). In PDH, the E1 subunit is a pyruvate decarboxylase, which catalyses the reductive acetylation of the lipoamide of the E2. The E2 subunit, an acetyltransferase, transfers the acetyl group to a molecule of CoA, resulting in the reduction of both sulfurs of the dithiolane ring. The amount of lipoamides on the same subunit varies from two to three in Gram-negative bacteria (de Kok et al., 1998). Lastly, the E3 subunit is a dihydrolipoamide dehydrogenase that oxidizes the reduced form of lipoamide, transferring the reducing equivalents to NAD^+, by using a FAD^+ cofactor as an electron acceptor (de Kok et al., 1998).

Gram-negative bacteria, such as rhizobia, possess PDH complexes with octahedral cores of 24 E2 subunits, associated with 12 E1 and 6 E3 subunits (Gao et al., 2002). In *S. meliloti*, the E1 and E2 subunit structure appears to be most similar to the Gram-negative bacteria *Zyomonas mobilis*: the E1β subunit contains a lipoyl domain in both species. However, the role of this lipoic acid is still unknown (Cabanes et al., 2000).

The genes encoding for the *S. meliloti* PDH complex have been identified and isolated.

The genes *pdhAα* and *pdhAβ* encoding for the E1 component, and *pdhB* encoding for the E2 component, constitute an operon. Usually *pdh* operons contain an *lpd* dihydrolipoamide dehydrogenase (E3) gene immediately downstream of the E1 and E2 genes (Cabanes et al., 2000). Instead, in *S. meliloti*, there is a palindromic sequence, which could be a transcriptional terminator followed by two open reading frames (ORFs) and an *lpdA1* gene encoding for E3 (Cabanes et al., 2000).

PDH is crucial for the growth on pyruvate or other carbon sources that get converted into pyruvate, as demonstrated by the glucose catabolic deficiency of the *B. subtilis* (Gao et al., 2006) and *Rhizobium leguminosarum* (Glenn et al., 1984) PDH mutants. Moreover, PDH has also an essential role in the anaplerotic reaction that converts malate into acetyl-CoA. Failure of a PDH mutant to grow on malate can be expected, as in the case of a *Pseudomonas aeruginosa* PDH mutant (Jeyaseelan and Guest, 1980). However, an alternative pathway to produce acetyl-CoA is possible, since a PDH mutant of *R. leguminosarum* grew on succinate (Glenn et al., 1984).

Regulation of the *pdh* operon has not yet been elucidated in *S. meliloti*. No sequence similar to the *E. coli* pyruvate-sensitive repressor (PdhR) binding site was found upstream of *pdhAα*. However, transcription of *pdhA* is enhanced under symbiotic conditions, and the addition of pyruvate induced the activity of the PDH complex of the free-living form of *S. meliloti* (Cabanes et al., 2000).

1.4.2 2-Oxoglutarate dehydrogenase complex (OGD)

In a similar fashion to the PDH, the OGD complex converts 2-oxoglutarate into succynil-CoA. The E1, 2-oxoglutarate dehydrogenase, and the E2, succinyl transferase, are encoded by

the genes *sucA* and *sucB* in *S. meliloti* (Capela et al., 2001). Downstream of these genes, is an *lpdA2* gene which, as *lpdA1*, encodes for dihydrolipoamide dehydrogenase.

The expression of the *S. meliloti* genes *sucA* and *sucB* is controlled by the same promoter that regulates the expression of the *mdh* gene for malate dehydrogenase and the subunits of the succynil dehydrogenase enzyme complex (Dymov et al., 2004). Apart from the copy in the chromosome, within the *mdh-sucCDAB* operon, *S. meliloti* contains a second gene for E2 (*SMb20019*) on pSymB, one of its two megaplasmids. Mutational analysis confirmed that the copy located on the chromosome, *sucB*, is crucial for the OGD function. Only when *sucB* was disrupted was the OGD activity completely knocked out and was the growth on glutamate as the sole carbon source reduced (M. Sc. Thesis, O. Trottier, 2008).

As opposed to *sucA* and *sucB*, which are co-transcribed in the *mdh-sucCDAB* operon, expression of *lpdA2* appears to be controlled by a different operon. Mutation in *S. meliloti* by gene fusion of one of the three ORFs upstream from *lpdA2*, *SMc02486*, a hypothetical short chain dehydrogenase/reductase, was found to have important polar effects on the expression of *lpdA2* (Jacob et al., 2008). The resulting mutant had a growth deficiency in most carbon sources assayed, including arabinose and glutamate. It is possible that these genes are in the same operon, and that a promoter site is located upstream of *Smc02486* (Jacob et al., 2008).

OGD activity is crucial for the growth on glutamate as the sole carbon source, since glutamate is converted into 2-oxoglutarate by glutamate dehydrogenase, which is usually used by OGD in the TCA cycle. Another OGD mutant of *S. meliloti* was isolated by Duncan and Fraenkel (1979). This strain was isolated through chemical mutagenesis with nitrosoguanidine, and was unable to grow on arabinose (catabolized to 2-oxoglutarate in *S. meliloti*) as the sole carbon

source (Duncan and Fraenkel, 1979). The mutation of the *sucA* gene of *R. leguminosarum* also decreased the activity of the OGD complex and increased the excretion of glutamate in this strain (Walshaw et al., 1997).

1.4.3 Branched chain α-keto acid dehydrogenase complex (BKD)

The BKD, the third member of the 2-oxo acid dehydrogenase family, has three types of subunits homologous to those of the previous complexes: a dehydrogenase (E1), a transacylase (E2), and a dihydrolipoamide dehydrogenase (E3). The BKD complex is common to the catabolism of valine, leucine and isoleucine. These amino acids are converted by various enzymes into three 2-oxo acids: 2-ketoisovalerate, 2-keto-3-methylvalerate, and 2-ketoisocaproate. BKD catalyses the conversion of these 2-oxo acids to their respective acyl-CoA derivatives: isobutyrul-CoA, 2-methylbutyryl-CoA, and isovaleryl-CoA (Massey et al., 1976). Finally these can be converted into acetyl-CoA and enter in the TCA cycle to be further oxidized (Lowe et al., 1983).

BKD is not naturally expressed in *E. coli*, although it has been thoroughly studied in *P. putida*, *P. aeruginosa* and *B. subtilis* (Sykes et al., 1987). In *P. putida*, BKD is induced by the presence of branched-chain keto acids and valine (Marshall and Sokatch, 1972). Moreover, mutants of BKD in *P. putida* and *B. subtilis* showed a simultaneous loss of ability to use any of the three branched-chain amino acids as sole carbon sources (Massey et al., 1976).

In *S. meliloti*, four genes have been found to share homology for genes encoding for the BKD subunits. The genes *bkdAα* and *bkdAβ* encode for the E1 component, and *bkdB* encodes for the E2 component (Galibert et al., 2001). In the same cluster and downstream of *bkdB* is the gene

lpdA3, encoding for a dihydrolpoamide dehydrogenase. The location of this *lpd* gene differs from that of the *lpdA1* and *lpdA2* genes which are in comparison very separated from the genes encoding for the other subunits.

Little is known about the BKD complex in rhizobia. However, the branched-chain amino acid biosynthesis, transport and role in the bacteroids have been intensively studied. In *R. leguminosarum*, failure to transport branched-chain amino acids into the cells produced ineffective symbiotic relationships with the plants, suggesting the bacteroids need the uptake of the plant-produced amino acids (Dunn et al., 2014; Prell et al., 2009). Disruption of the branched-chain amino acid transport genes in *S. meliloti* did not affect the symbiotic relationship as it did with *R. leguminosarum*, suggesting that *S. meliloti* is not as dependant of the plant amino acid supply as *R. leguminosarum*. However, when the genes involved in leucine synthesis were disrupted in *S. meliloti*, the strains became leucine auxotrophs and would not fix nitrogen as bacteroids (Dunn et al., 2014).

1.5 Dihydrolipoamide dehydrogenases

Dihydrolipoamide dehydrogenases (LPDs) are functional components of the OADHCs and other multimeric enzymes (e.g. glycine cleavage complex, GCV; Steiert et al., 1990). LPDs are members of the NAD^+ oxidoreductases enzyme family, which includes glutathione reductases, mercuric reductases, and trypanothione reductases. LPDs catalyze the oxidation of dihydrolipoamide to lipoamide, replenishing the functionality of the lipoyl domain of the neighbouring subunit. More specifically, LPD catalyzes the oxidation of a dithiol group to a disulfide bond, transferring a proton via an FADH cofactor to NAD^+.

LPDs are found in a wide range of species since it constitutes a subunit of multi-enzyme complexes commonly involved in aerobic metabolism. The enzymological properties and structural characteristics of the LPDs from *E. coli* and *Azotobacter vinelandii* have been intensively studied (Schwind et al., 2001). As for the genes for LPD, different variants have been cloned and sequenced in several organisms (Schwind et al., 2001). In most prokaryotes, a single gene expressed under the control of a unique promoter encodes for an LPD shared by multiple complexes. That promoter can be one of the PDH operon (*E. coli, Haemophilus influenzae* and *B. subtilis*) or the OGD operon (*A. vinelandii* and *P. fluorescens*; de Kok et al., 1998).

Documented exceptions to a single gene occurrence are *P. putida* and *Ralstonia eutropha*, having three and two copies of this gene respectively. In *R. eutropha*, one gene for LPD (*pdhL*) is present in the PDH operon, and a second gene (*odhL*) is located in the OGD cluster (Hein and Steinbüchel, 1996). In *P. putida*, a single *lpdG* located in the OGD operon, encodes for the LPD component of both the PDH and the OGD complexes, as well as the L-factor for the GCV complex (Palmer et al., 1991). A second LPD (*bkdC*), found in the BKD operon of *P. putida*, specifically binds to the E1 and E2 subunits of BKD (Sokatch et al., 1981). Finally, there is a third gene unrelated to any operon in *P. putida* that could partially substitute for LPD in the PDH and the OGD complexes when *lpdG* is missing (Palmer et al., 1991).

Another exception of the single-gene encoded LPD is *S. meliloti*, in which three genes (*lpdA1*, *lpdA2* and *lpdA3*) homologous to the *E. coli lpd* gene have been identified (Figure 3). Unlike in *P. putida*, each of these genes is proximal to the genes encoding the subunits of a different complex. The *lpdA1* gene in *S. meliloti,* as in *E. coli* and *B. subtilis*, is located downstream of the gene encoding for the E2 of PDH, but it is separated from the cluster by two

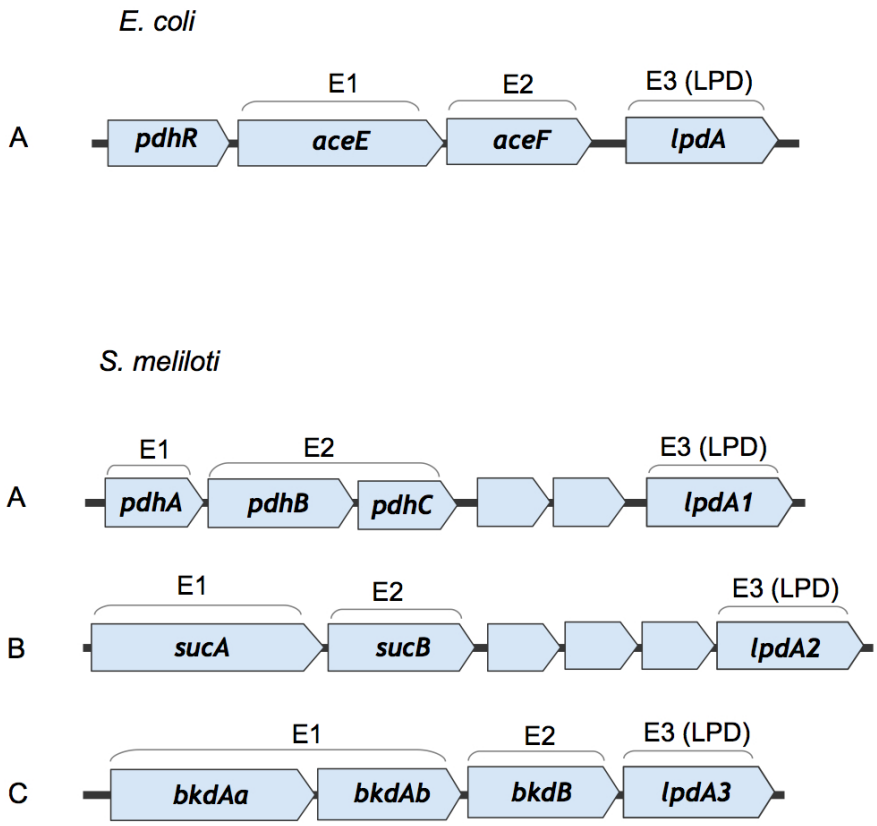

Figure 3: Graphic representation of the PDH (A), OGD (B), and the BKD (C) gene arrangements in *E. coli* and *S. meliloti*. The E1, E2 and E3 subunits of each complex are indicated with brackets (Quail et al., 1994; Capela et al., 2001). The size of the genes is not to scale.

ORFs (Capela et al., 2001; Soto et al., 2001). The first ORF (*ada*) is a gene encoding for an arylesterase. This gene is coexpressed with the *lpdA1*, and its disruption produced a PDH mutant phenotype (Soto et al., 2001).

The *lpdA2* gene is located three ORFs downstream of the *mdh-sucCDAB* operon, which encodes for malate dehydrogenase, succinyl-CoA synthtase, and the E1 and E2 subunits of the OGD complex (Capela et al., 2001). Lastly, the *lpdA3* gene is found directly downstream of *bkdB* in the BKD operon (Capela et al., 2001). These genetic dispositions suggest a relationship between the subunits and their function in a specific complex (Figure 3).

2 Hypothesis and Objectives

The *lpdA1*, *lpdA2* and *lpdA3* genes of S. meliloti are proximal to the genes encoding for the E1 and E2 subunits of the PDH, OGD and BKD complexes, respectively (Figure 3). We hypothesized that in *S. meliloti* the LPDs expressed from the *lpdA* genes are interchangeable between the different complexes.

The goals of this thesis were:

- to isolate mutants of *S. meliloti* with stable transposon insertions in the three *lpdA* genes;
- to clarify the function of these *lpdA* genes towards the PDH, OGD and BKD complexes;
- to determine whether the *lpdA1*, *lpdA2* and *lpdA3* products are interchangeable between the different complexes, and if they are; to which extent;
- to test if the knockout of the separate genes had an effect on the N_2-fixation process of the bacteroids.

3 Materials and Methods

3.1 Strains, plasmids and transposons

The following work made use of the bacteria, plasmids and transposons listed (Table 1).

3.2 Media and culture conditions

The bacterial strains were obtained from frozen DMSO stocks kept at -80 ºC. After incubation, *E. coli* at 37 ºC and *S. meliloti* at 30 ºC, individual colonies were used to inoculate media or streak plates (Table 2). Frozen permanent stocks were made of a TY grown overnight culture suspended in TY, and 7% DMSO. For the isolation of new strains, single colonies were streak purified twice previously to making a DMSO stock.

When culturing *S. meliloti* on liquid LB medium, this was supplemented with 2.5 mM $MgSO_4$ and 2.5 mM $CaCl_2$ (LBmc). Antibiotics also supplemented media when selecting for a marker (Table 3).

3.3 Total genomic DNA isolation

This technique was used for total genomic DNA isolation of *S. meliloti* (Meade et al., 1982). A 10 mL overnight culture was washed first with 5mL ice-cold 0.85% NaCl, resuspended in 5 mL ice-cold TES (10 mM Tris pH 7.8, 25 mM EDTA pH 8, 150 mM NaCl) and then pelleted. The pellet was frozen at -20 ºC and later resuspended in 2.5 mL of ice-cold $T_{10}E_{25}$. Lysozyme (0.25 mL of 2 mg per mL $T_{10}E_{25}$) was added and the suspension incubated for 15 minutes in a 37 ºC water bath. To this solution, 0.35 mL of autodigested sarkosyl-protease

Table 1: Bacterial strains used in the extent of the study.

Strain, plasmids, transposons	Properties	Reference
Sinorhizobium meliloti		
Rm1021	SU47 str-21, Sm^r	Meade et al., 1982
Rm30360	Rm1021 *lpdA2*172::EZ-Tn5<KAN-2>	This study
Rm30368	Rm1021 *lpdA1*1084::EZ-Tn5<TET-1>	This study
Rm30049	Rm1021 *mdh*448::Tn5tac1	Dymov et al., 2004
Rm30277	RmG212::Tn5-B20, Sm^r, Nm^r, ara^-, pyr^-, $glut^-$, $GABA^-$, suc^-, ace^-, $X\text{-}gal^+$	Laboratory strain
Escherichia coli		
EcDH5α	*supE44, hsdR17, recA1, thi-1, endA1, lacZα, gyrA96, relA1*	Hanahan, 1983
Ec10615	EcDH5α pMS1	This study
Ec10616	EcDH5α pMS2	This study
Ec10617	EcDH5α pMS3	This study
Ec10628	EcDH5α pMS202	This study
Ec10644	EcDH5α pMS5	This study
Ec10651	EcDH5α pMS101	This study
Ec10657	EcDH5α pMS13	This study
Ec10664	EcDH5α pMS303	This study
Ec10671	EcDH5α pMS18	This study
EcMT616	EcMT607 pRK600	Finan et al., 1986
Ec10597	EcDH5α pBM1	Babic, 2010
Ec10606	EcDH5α pBM2	Babic, 2010
Plasmids		
pGEMT-easy	PCR cloning vector, Amp^r	Promega
pMS1	pGEM-T Easy carrying *lpdA1* whole gene, Amp^r	This study
pMS2	pGEM-T Easy carrying *lpdA2* whole gene, Amp^r	This study
pMS3	pGEM-T Easy carrying *lpdA3* whole gene, Amp^r	This study
pMS202	pMS2, *lpdA2*172::EZ-Tn5<KAN-2>, Amp^r, Kan^r, Nm^r	This study
pMS101	pMS2, *lpdA1*1084::EZ-Tn5<TET-1>, Amp^r, Tc^r	This study
pMS303	pMS3, *lpdA3*::EZ-Tn5<DHFR-1>, Amp^r, Tmp^r	This study
pJQ200SK	Suicide cloning vector carrying *sacB*, Gm^r	Quandt and Hynes, 1993
pMS5	pJQ200-SK carrying NotI fragment of pMS202, Gm^r, Kan^r, Nm^r	This study
pMS13	pJQ200-SK carrying NotI fragment of pMS101, Gm^r, Tc^r	This study
pMS18	pJQ200-SK carrying NotI fragment of pMS303, Gm^r, Tmp^r	This study
pLAFR1	IncP cosmid cloning vector, Tc^r	Friedman et al., 1982

Table 1 (continued): Bacterial strains used in the extent of the study.

Strain, plasmids, transposons	Properties	Reference
pBM1[Bank]	pLAFR1 carrying *S. meliloti* genomic DNA fragment with *lpdA1*	Friedman et al., 1982
pBM2[Bank]	pLAFR1 carrying *S. meliloti* genomic DNA fragment with *lpdA2*	Friedman et al., 1982
pRK600	*In trans* mobilizing vector	Finan et al., 1986
Transposons		
EZ-Tn5<KAN-2>	*In vitro* transposable element, Kan^r, Nm^r	Epicentre Biotech.
EZ-Tn5<TET-1>	*In vitro* transposable element, Tc^r	Epicentre Biotech.
EZ-Tn5<DHFR-1>	*In vitro* transposable element, Tmp^r	Epicentre Biotech.

Table 2: Composition of the media used in this study.

Medium	Composition
LB (Sambrook et al., 1989)	5 g/L NaCl, 5 g/L Yeast Extract, 10 g/L Tryptone, and 15 g/L agar for agar plates
LBmc	LB, 2.5 mM $CaCl_2$ and 2.5 mM $MgSO_4$
M9 (Sambrook et al., 1989)	50 mL/L 20X M9 salts, 1mM MgSO4, 0.25 mM $CaCl_2$, 1 mg/L Biotin and 15 g/L agar for plates 20X M9 salts: 11.6 g/100 mL Na_2HPO_4, 6 g/L KH_2PO_4, 1 g/100 mL NaCl, 2 g/100 mL NH_4Cl, autoclaved separately from agar, MgSO4 and $CaCl_2$
TY (Sambrook et al., 1989)	5g/L NaCl, 3g/L Yest Extract

Table 3: Media antibiotic supplements and their concentration.

Antibiotic	Stock solution (mg/mL)	Final concentration (µg/mL)
Gentamycin (Gm)	6	20
Ampicillin (Amp)	10	100
Neomycin (Nm)	40	200
Streptomycin (Sm)	40	200
Kanamycin (Km)	6	20
Chloramphenicol (Cm)	2	10
Rifampicin (Rf)	5	25
Tetracycline (Tc)	2	2, 10*

* 2 µg/mL for *S. meliloti* and 10 µg/mL for *E. coli.*

solution (5 mg pronase E in $T_{10}E_{25}$ incubated 2 hours at 37 ºC) was pipetted in, and the incubation continued for another 30 minutes. An equal volume of phenol was added and mixed with the solution. Removal of the top aqueous solution containing the DNA was possible after centrifugation (15 minutes at 5000 rpm). This step was repeated until there was no or little cell debris at the interphase. Following the phenol extraction, two more chloroform extractions were made. A final concentration of 0.3 M of NH_4-acetate was reached using a 5 M stock solution. Adding 1 mL of isopropanol caused DNA to precipitate. The DNA was removed by sticking it to the tip of a sterile pasteur pipette, and washed by dipping it into 0.5 mL of 70% ethanol and 95% ethanol. The DNA was then left to air-dry for some minutes, before dissolving it in 0.5 mL of $T_{20}E_1$. For complete dissolution, the DNA solution was incubated 20 minutes at 65 ºC.

3.4 Boiling method for plasmid DNA isolation

This method was modified from Holmes and Quigley (1981), and was used for rapid plasmid extractions from *E. coli* strains. For this purpose, 1.5 mL of overnight culture was pelleted (1 minute at 13,000 rpm) and resuspended in 0.35 mL of STET (8 % sucrose, 0.5% Triton X-100, 50 mM EDTA pH 8, 50 mM Tris pH 8). After the addition of 10 µL of lysozyme (50 mg/mL in 10 mM Tris pH 8) the tubes were transferred to a boiling water bath for 3 minutes. Next, the tubes were centrifuged 15 minutes at 13,000 rpm at RT. The pellet had a viscous consistence and could be removed with a wooden stick. To precipitate the DNA , 0.33 mL of cold isopropanol was added to the supernatant, and the solution incubated at -80 ºC for 15 minutes. The DNA was pelleted by centrifugation (15 minutes at 13,000 rpm), and washed with 70% and 95% ethanol, consecutively. Once the ethanol evaporated, the pellet was resuspended in 50 µL of

10 mM Tris pH 8. To remove residual RNA, the DNA solution was mixed with 1 µL of RNase (1 mg/mL stock) and incubated 20 minutes at 37 ºC.

3.5 Large scale alkaline plasmid extraction and purification

An alkaline lysis method was used for large scale plasmid extractions (Sambrook et al., 1989). An overnight 500 mL culture of *E. coli* was washed with 200 mL sterile saline solution and resuspended in 10 mL of Solution I (50 mM glucose, 25 mM TrisCl, pH 8, and 10 mM EDTA, pH 8). To this suspension, 1 mL of freshly prepared lysozyme solution (10 mg/mL in 10 mM TrisCl, pH 8) and 20 mL of Solution II (0.2 M NaOH, 1% SDS) were added, and mixed gently by inversion. After incubating for 10 minutes at RT, 15 mL of Solution III were added (5 M potassium acetate, 11.5% v/v glacial acetic acid). The suspension was mixed thoroughly by shaking until a white precipitate formed, and then stored at -20 ºC until needed.

The mixture with the bacterial lysate was centrifuged at 4000 rpm for 15-30 minutes at 4 ºC until a tight pellet was formed. The supernatant was filtered through four layers of cheesecloth into a clean bottle and mixed with 0.6 volume of isopropanol. After 10 minutes incubating at RT, the bottle was centrifuged at 5000 rpm for 15 minutes at RT. The resulting pellet was washed with 70% ethanol, air dried and resuspended in 3 mL 10 mM Tris (pH 8).

To achieve sequencing quality requirements, plasmid DNA was purified by the polyethylene glycol method. An equal volume of ice-cold 5 M LiCl solution was mixed with the DNA solution, and then centrifuged at 10 000 rpm for 10 minutes at 4 ºC. Next the supernatant was decanted onto a clean tube and mixed thoroughly with an equal volume of isopropanol, to centrifuge afterwards at 10 000 rpm for 10 minutes at RT. The resulting pellet was cleaned with

70% ethanol, air dried, and resuspended in 500 µL of TE (pH 8) with RNase (20 µg/mL). The suspension was then left to incubate at RT for 30 minutes before mixing with 500 µL of 1.6 M NaCl containing 13% (w/v) polyethylene glycol. After a 5 minutes centrifugation at 13 000 rpm, the obtained pellet was resuspended in 400 µL of TE (pH 8), and to this suspension, one extraction of phenol, one of phenol:chloroform, and a last one of chloroform were done. The resulting aqueous phase was transferred to a new tube and 100 µL of 10 M ammonium acetate were added, mixed, and combined with two volumes of 95% ethanol. After a 10 minute incubation at RT, the suspension was centrifuged at 13 000 rpm for 5 minutes. The resulting pellet was then washed with 70% ethanol, air dried and resuspended in 500 µL of 10 mM Tris (pH 8).

3.6 Polymerase chain reaction (PCR)

PCR was often used to amplify the *lpdA* genes and the plasmid insertions. Standard TAQ polymerase and other reagents for PCR were purchased from Bioshop (Burlington, Ontario) or Life Technologies Inc. (Mississauga, Ontario). The program set on the PTC-100 thermocycler (MJ Research, Watertown, MA, USA) started with a denaturation step at 95 ^{o}C for 5 minutes, followed by 35 cycles of the following stages: a denaturation step at 95 ^{o}C for 30 seconds, an annealing step for 45 seconds, and an extension step at 72 ^{o}C for 45 seconds. After the 30 cycles, a last extension step was set for 10 minutes at 72 ^{o}C. The temperature of the annealing step differed according to the primers used (Table 4).

Table 4: Primers used in this study and temperatures used in the annealing step of the PCR.

Primers	Sequence	Amplicon size	PCR Annealing T
lpdA1 fwd	CGA AGA CAG CAG AAA ACA CGA CTG	1445	60 °C
lpdA1 rev	TGA GAA CCT CCC CGC ATT GTA G		
lpdA2 fwd	TCC GAC AAG GCG ACT TAC G	1406	60 °C
lpdA2 rev	AAT GCG GGG TTC AGT TGG		
lpdA3 fwd	GGC GCT GAT TTT CGT TGA AGG A	1395	60 °C
lpdA3 rev	CGG TGA ATC CGG GAT TCA GTT		
SP6	ATT TAG GTG ACA CTA TAG AA	NA	55 °C
T7	TAA TAC GAC TCA ACT ATA GGG		
pJQ200-SK fwd	TGG CGA AAG GGG GAT GTG CT	NA	55 °C
pJQ200-SK rev	GCA CGA CAG GTT TCC CGA CT		
pLAFR1 fwd	CGC CTC GAT CAG CTC TTG CAC	NA	55 °C
pLAFR1 rev	GGT GCT GGC ATC GAC TTT CA		

3.7 Agarose gel electrophoresis

When evaluating the quality and size of DNA, 0.8% agarose gels were used. The agarose was dissolved in TAE buffer (40 mM Tris, pH 7.6, 20 mM acetic acid, 1 mM EDTA; Sambrook and Russel, 2001). Gels were stained with RedSafe Nucleic Acid Staining Solution (Intron Biotechnology, Seongnam, Korea). The bands were visualized with a Syngene Chemi Genius Bio Imaging System (Cambridge, United Kingdom).

3.8 DNA restriction digest

For the plasmid digest, restriction endonucleases obtained from Technologies Inc. or Bioshop were used, and all their reactions carried out as described in the product manual.

3.9 Sequencing and sequence analysis

Plasmid inserts were sequenced by the Sanger Sequencing method (Sanger et al., 1977) at the McGill University and Génome Québec Innovation Centre (Montreal, Québec, Canada). Sequence analysis was performed using the IANT (integrated Annotation Tool) web-based semiautomated annotation environment of the *S. meliloti* sequence (http://iant.toulouse.inra.fr; Capela et al., 2001), as well as the tools MacVector version 7.2 (MacVector, Inc., Cary, North Carolina, USA), and Sequencher version 4.7 (Gene Codes Corp., Ann Arbor, Michigan, USA).

3.10 DNA ligation

Ligation of the PCR products into pGEM-T Easy vector (Promega Corportation, Madison, Wisconsin) was done as described in the kit's manual. The ligation mixture was

incubated overnight at 4 ºC, and then directly transformed into *E. coli* DH5α. Selection of transformants was done on LB agar supplemented with Amp, X-gal and IPTG. Transformants were screened for the correct insert through colony PCR using the primers SP6 and T7 (Table 4).

When ligating fragments to the vector pJQ200SK, both vector and plasmid containing the insert of interest were restricted with *Not*I. The restriction digest products were heated 20 minutes at 65 ºC to inactivate the enzyme. To precipitate the DNA, the suspension was adjusted to 0.3 M sodium-acetate, homogenized thoroughly, and mixed with two volumes of ice cold ethanol or isopropanol. The solution was stored at -20 ºC for 20 minutes, and then centrifuged 10 minutes at 13,000 rpm to recover the DNA. The pellet was consecutively washed with 70% and 95% ethanol, air dried and finally dissolved in $T_{10}E_1$. Ligation was carried out by T4 DNA Ligase (Life Technologies Inc.) with a molar ratio of 3:1 of insert DNA over the vector, and incubated in a RT water bath that was then placed in a refrigerator overnight. Transformants were screened for the correct insert through colony PCR using the primers flanking the pJQ200SK multiple cloning site (Table 3).

3.11 Transposon EZ-Tn5 mutagenesis

Plasmids isolated with the QIAprep Spin Miniprep Kit (QIAGEN, Toronto, Ontario) were mutagenized using the EZ-Tn5 <TET-1> Insertion Kit, EZ-Tn5 <KAN-2> Insertion Kit, and the EZ-Tn5<DHFR-1> Insertion Kit (Epicentre, Madison, Wisconsin). The reaction product was transformed into *E. coli* DH5α cells, which were plated on LB supplemented with vector and the transposon marker. Transformants were screened through colony PCR using the primers flanking the vector's multiple cloning site.

3.12 Generation of calcium competent *E. coli* DH5α cells

A 100 mL of LB with 15 mM glucose was inoculated with 1 mL of an overnight culture of *E. coli* DH5α. The culture was incubated at 37 ºC with a shaking speed of 180 rpm until an OD_{600} of 0.5-0.6 was reached. Immediately after, the flask was placed on ice for 10 minutes, occasionally shaking it to ensure that cooling occurred evenly and quickly. The culture was centrifuged at 5000 rpm for 5 minutes at 4 ºC and the pellet was gently resuspended in a total volume of 40 mL of ice cold solution A (100 mM $CaCl_2$), incubated on ice for 1 hour then centrifuged at 4000 rpm for 10 minutes at 4 ºC. The pellet was resuspended in 4 mL of solution B (100 mM $CaCl_2$, 10% glycerol) and stored as 200 µL aliquots at -80 ºC.

3.13 Competent cell transformation

The competent *E. coli* DH5α cells were thawed on ice for 15 minutes. An aliquot of 50 µL was gently mixed with 2.5 µL of plasmid DNA and left on ice for 30 minutes. After incubation, the cells were heat shocked at 42 ºC for 90 seconds, and chilled again on ice for 60 seconds, then 1 mL of pre-warmed (37 ºC) LB medium was added. The tube was left to incubate for 45 minutes in a 37 ºC water bath, then centrifuged for 10 minutes at 5000 rpm, the supernatant was discarded, and 100 µL of LB medium added to resuspend the pellet and spread the cells onto an LB plate with the selective antibiotics. Transformed colonies appeared after 24-48 hours of incubation at 37 ºC and were purified twice by single colony isolation.

3.14 Triparental mating of a plasmid from *E. coli* into *S. meliloti*

The mobilizing strain MT616 was used to conjugate plasmids lacking *tra* genes from *E. coli* into *S. meliloti* (Finan et al., 1986). All cultures were first washed twice in sterile saline then 1 mL of each culture was pelleted and resuspended in 100 µL of LB. From these concentrated cultures 15 µL of the *E. coli* donor strain, 15 µL of the *E. coli* MT616 helper strain and 45 µL of the *S. meliloti* recipient strain were combined in an Eppendorf tube. This mixture was placed as a single droplet in the middle of an LB plate and incubated overnight at 30 ºC. Equal amounts of each strain were also spotted individually for pairwise controls. Following the incubation, the bacterial mass was scraped from the plate and resuspended in 1 mL sterile saline. A serial dilution was made from this suspension and 100 µL from each of the dilutions were plated on LB plates with antibiotics. For the pairwise controls, only the undiluted cells were plated. Transconjugant colonies were visible after 2-7 days of incubation at 30 ºC and were purified three times by single colony isolation.

3.15 General transduction of *S. meliloti*

Phage stock

From an overnight *S. meliloti* culture grown on LBmc, 0.5 mL were removed and combined with 4.5 mL of pre-warmed (30 ºC) LBmc. To this, 20 µL of a bacteriophage ΦM12 (Finan et al., 1984) were added and the mixture incubated 8-12 hours on a wheel. Next, 250 µL of chloroform were added to the suspension, followed by a gentle vortex, and then incubated overnight at 4 ºC without disturbance. The top layer (1-2 mL) was centrifuged 5 minutes at 4000 rpm, and the supernatant stored until at 4 ºC needed.

Phage titre calculation

Ten-fold serial dilutions were made from the phage stock using LBmc. From each dilution, 100 µL were mixed with 100 µL of an overnight *S. meliloti* culture. After 20 minutes at RT, 2.5 mL of LBmc 0.8% agar were added, and poured onto pre-warmed (37 ºC) LBmc plates. When solidified, the plates were incubated overnight at 30 ºC, and the formed plaques counted. As controls one plate contained soft agar with *S. meliloti*, and another plate soft agar with solely a phage dilution.

Transduction

The phage stock was diluted 1:20 or 1:40, depending on the concentration necessary to reach a multiplicity of infection (MOI) of 0.5. From this dilution, 1 mL was taken and gently mixed with 1 mL of overnight recipient *S. meliloti* culture. After 20 minutes, 2.5 mL of sterile 0.85% saline solution were added, and the whole suspension centrifuged for 5 minutes at 4000 rpm. The supernatant was discarded and the step with saline solution repeated. Finally, the resulting pellet was resuspended in 1 mL saline, and then 100 µL plated on LBM9 with Nm or Tc, depending on the selectable marker of the strain. Controls were done by plating separately the diluted phage and the recipient culture on the selective media.

3.16 Growth rates

The carbon usage capability was initially evaluated by streaking the bacteria on M9 agar plates with sole carbon sources and recording the apparition or not of colonies after seven days of incubation at 30 ºC.

For the making of growth curves, flat-bottom 24-well transparent plates (Costar, Corning Incorpated Life Sciences, Tewksbury, Massachusetts) were used containing 1.5 mL/well of M9 minimal media with 15 mM of either arabinose, glucose, glutamate, malate or succinate. Cultures were grown in LBmc to an OD_{600} of 1, washed twice with sterile saline solution (0.85% NaCl), resuspended in 1 mL of M9 containing the tested carbon source and 0.2 mL used to inoculate the corresponding carbon-source wells of the microplate. The plates were incubated in a microplate reader (Infinite 200 PRO, Tecan, Maennedorf, Switzerland) at 30 ^{o}C with an orbital shaking amplitude of 4 mm, and the optical density recorded every 15 minutes. All samples, including the blanks, were done in triplicates.

Growth rates were obtained using the next formula:

$$k = ((\log_{10} A - \log_{10} A_0)\, 2.303) / (t - t_0)$$

where k is the growth rate coefficient (h^{-1}), A is the OD_{600} of the culture at time t, and A_0 the OD_{600} at time t_0.

3.17 Southern blot hybridization

The probes were generated by non-radioactive random primed DIG-labeling of pMS1 and pMS2 with Klenow enzyme following the Roche protocol guide (The DIG system user's guide for filter hybridization, Boehringer Mannheim/Roche Diagnostics, Laval, Quebec). The genomic DNA of each strain was digested by *Eco*RI and run on an agarose gel. The steps following gel electrophoresis (southern transfer, depurination, denaturation, neutralization, blotting, and fixation) were performed according to the DIG system user's guide. The DNA was blotted onto a positively charged nylon membrane (Roche Life Sciences, Brandford, Connecticut) via upward

capillary transfer using the Whatman 3MM filter paper wick setup method (Brown, 2001), and immobilized on the membrane by UV crosslinking (1200 μJ [x100], UV Stratalinker 1800, Stratagene, La Jolla, California). A colorimetric detection system based on nitroblue tetrazolium (NBT) and 5-bromo-4-chloro-3-indolylphosphate (BCIP) was used to visualize the probes hybridized to the blotted genomic DNA of the *S. meliloti* strains.

3.18 Crude cell extract

The *S. meliloti* cultures were grown on M9 minimal media, supplemented with 1% LB and with either 15 mM arabinose or 15 mM succinate. An Erlenmeyer flask containing 500 mL of media were inoculated with 5 mL of overnight culture grown on LBmc, previously pelleted and resuspended in an equal volume of fresh LB medium.

Once it reached an OD_{600} of 0.8-1 the cultures were centrifuged at 5000 rpm for 15 minutes at 4 ^{o}C. The pellet was washed twice with 200 mL of washing buffer (20 mM Tris HCl, pH 7.8, 1 mM $MgCl_2$) and stored at -20 ^{o}C until sonication. Thawed pellets were resuspended in sonication buffer (4 mL/g pellet wet weight; 20 mM Tris HCl, pH 7.8, 1 mM $MgCl_2$, 10 mM β-mercaptoethanol, 10% glycerol) and transferred into 50 mL plastic tubes and sonicated on ice five times for 5 seconds at 90 Watt, using the Sonifer Cell Disruptor W185D (Heat Systems – Ultrasonics inc., Plainview, New York, USA), with 5 minutes of cooling on ice between sonications. The sonicated suspensions were centrifuged for 20 minutes at 9000 rpm at 4 ^{o}C and the supernatant was then decanted onto a clean tube and stored at -20 ^{o}C.

The protein concentration of the extracts was determined by a Bradford assay, using bovine serum albumen as the protein standard. Briefly, 1 mL of BioRad protein assay dye (Bio-

Rad Laboratories, Mississauga, Ontario) was mixed with 20 μL of the crude protein extract and incubated at RT for 5 minutes before measuring its absorbance at 595 nm. Samples were done in triplicate, and the average values used for the calculation of the standard curve and the protein content.

3.19 Enzyme assays

To measure specific activity, the absorbance of NADH produced during the enzyme assay reaction was measured at 340 nm (Ultrospec 2000 Spectrophotometer, Pharmacia Biotech, Uppsala, Sweden). Each assay was done in triplicates, and the specific activity was calculated using the formula:

$$SA = \frac{\Delta\text{Absorbance x reaction volume (mL)}}{\text{time (min) x protein (mg) x } \varepsilon}$$

where ΔAbsorbance equals to the average slope of the absorbance versus time curve, and ε is the extinction coefficient of NADH at 340 nm to convert ΔAbsorbance to nmols (ε_{340}= 6.22 x 10^{-3} $nmol^{-1}$). Units for SA are nmol · min^{-1} · mg $protein^{-1}$. Standard error was calculated with the formula:

$$SE = \frac{SD}{\sqrt{n}}$$

where SD is the standard deviation and n the number of replicates (3 for each assay).

3.19.1 Malate dehydrogenase

$$\text{L-Malate} + NAD^+ \leftrightarrow \text{Oxaloacetate} + NADH + H^+$$

The malate dehydrogenase activity was measured using the method from Englard and Siegel (1969). This assay included 100 mM glycine-NaOH (pH 10), 85 mM L-malate, and 2.5 mM NAD^+ in a total volume of 1 mL. The reaction was initiated by the addition of 0.1 mg of protein.

3.19.2 2-Oxoglutarate and pyruvate dehydrogenases

$$\text{Pyruvate} + NAD^+ + \text{CoA-SH} \leftrightarrow \text{Acetyl-CoA} + NADH + CO_2$$

$$\text{2-Oxoglutarate} + NAD^+ + \text{CoA-SH} \leftrightarrow \text{Succinyl-CoA} + NADH + CO_2$$

The activity of OGD and PDH, was measured by the method of Reed and Mukherjee (1969). The reaction mixture of these assays contained: 50 mM phosphate buffer (pH 7.4), 1 mM $MgCl_2$, 3 mM L-cysteine, 2 mM NAD^+, 0.2 mM TPP and 0.1 mg of protein, in a total volume of 0.97 mL. The reaction was started by the simultaneous addition of 0.02 mL of 3 mM CoA trilithium salt trihydrate, and 0.01 mL of 0.1 M 2-oxoglutarate or 0.1 M sodium-pyruvate.

3.20 Plant growth evaluation

The set up used for plant growth was as described previously (Leonard, 1943). Briefly, a plastic pot was placed on a 500 mL beaker, with a cotton wick connecting the inside of the pot with the base of the beaker and a cotton layer covering the rest of the holes in the pot. The pots were filled with a nitrogen-free sand/vermiculite mixture (2:1 v/v) and the beakers with 250 mL

of Jensen's medium. The space between the pot and the beaker was covered with a double layer of aluminium foil and attached with electrical tape. The pots were covered with aluminium foil and autoclaved for at least 4 hours. Jensen's medium (Jensen, 1942) contained per litre: 1 g $CaHPO_4$, 0.2 g K_2HPO_4, 0.2 g $MgSO_4$, 0.2 g NaCl, 0.1 g $FeCl_3$, and 1 mL of trace minerals solution. The medium was prepared as 2X solution and adjusted to pH 7 before diluting it to 1X. The trace mineral solution had per 100 mL: 0.1 g H_3BO_3, 0.1 g $ZnSO_4$, 0.05 g $CuSO_4$, 0.05 g $MnCl_2$, 0.1 g Na_2MoO_4, 1 g Na_2EDTA, 0.2 g NaFeEDTA, and 0.04 g biotin.

Alfalfa seeds (*Medicago sativa* cultivar Iroquois, source: Cayuga Ontario Co-Op) were surface sterilized in 95% ethanol for 5 minutes, then 20 minutes in 2.5% sodium hypochlorite and then neutralized with a short rinse with sterile LB and repeated rinses of sterile water for over an hour.

Once surface sterilized, the seeds were placed on a water agar plate (1.5% agar in dH_2O) equidistantly one from each other, and incubated in the dark for 2 days at RT. Seeds that had germinated were transferred into a pot. The pots, with ten seedlings each, were incubated with a foil cover in a Conviron E15 plant-growth chamber (Winnipeg, Manitoba) programmed with a cycle of 16 hours of light at 25 ^oC, and 8 hours of darkness at 20 ^oC. Two days later, the foil cover was removed and the pots were inoculated. The inoculum consisted in 0.2 mL of overnight *S. meliloti* culture diluted in 10 mL of sterile dH_2O. Each pot treatment was done in triplicate, using independent cultures for each inoculum. Plants were grown for a total of four weeks and watered when needed using sterile dH_2O.

The plants were cut at the base of the stem where the colour changed from white to pale-pink or green. The shoots were stored and dried for at least 4 weeks at 50 ^oC and then weighed.

Leaf N and C concentrations (%) were measured using an Elemental Analyzer (NC2500 Elemental Analyzer, ThermoQuest Italic S.P.A., Italy) from oven-dried, ground samples.

4 Results

4.1 Construction of *S. meliloti lpdA* mutants

The first goal of this project was to isolate mutants of *S. meliloti* with stable transposon insertions in the three *lpdA* genes. To accomplish this we chose three derivatives of transposon Tn5: EZ-Tn5<TET-1> for *lpdA1*, EZ-Tn5<KAN-2> for *lpdA2*, and EZ-Tn5<DHFR-1> for *lpdA3*. Having different selectable markers in each gene would make it possible to attempt to isolate strains with mutations in more than one *lpdA* gene in the future. The three *lpdA* genes were each amplified by PCR, ligated into the pGEM-T Easy and transformed into *E. coli* DH5α. This resulted in the strains Ec10615, Ec10616 and Ec10617 carrying plasmids pMS1 (*lpdA1*), pMS2 (*lpdA2*) and pMS3 (*lpdA3*), respectively. The plasmids were mutagenized *in vitro* with the transposable elements (pMS1 with EZ-Tn5<TET-1>, pMS2 with EZ-Tn5<KAN-2>, and pMS3 with EZ-Tn5<DHFR-1>) and transformed into *E. coli* DH5α (Figure 4a). Multiple isolated colonies were screened by colony PCR for transposon insertions in the respective *lpdA* gene. One plasmid from each mutated *lpdA* was isolated and sequencing localized the insertion site of the transposon: *lpdA1*1084::EZ-Tn5<TET-1> in pMS101, *lpdA2*172::EZ-Tn5<KAN-2> in pMS202, and transposition of *lpdA3*508::EZ-Tn5<DHFR-1> in pMS303.

These plasmids were digested with *Not*I and the fragment containing the mutagenized *lpdA* genes were ligated into the suicide vector pJQ200SK (Figure 4b), resulting in the plasmids pMS13 (with *lpdA1*1084::EZ-Tn5<TET-1>), pMS5 (with *lpdA2*172::EZ-Tn5<KAN-2>) and

pMS18 (with *lpdA3*508::EZ-Tn5<DHFR-1>). The suicide vectors containing the mutagenized genes were conjugated from *E. coli* DH5α into Rm1021 via triparental mating (Figure 4c). Colonies of *S. meliloti* arising from the selection on LB 5% sucrose and the transposon marker (Tc, Nm, or Tmp), but also sensitive to Gm, represented gene replacement by double recombination events and thus mutants of the corresponding *lpdA* gene (Figure 4d).

To isolate *lpdA1* mutants, a two step selection process was done; first the mating spot was scraped up and incubated overnight into liquid LBmc enriched with HB and Tc, then the cells were plated on LB containing sucrose, Tc and HB. To isolate *lpdA2* mutants, the mating spot was directly plated on selective media, LB containing sucrose and Nm. The construction of a *S. meliloti lpdA3*508::EZ-Tn5<DHFR-1> mutant was not possible since no colonies could be isolated due to the high background of Rm1021 growth in the Tmp selecting media. Experiments of this study were performed with Rm30360 (*lpdA2*) and Rm30368 (*lpdA1*), however using the same procedure, other *lpdA2* mutants (Rm30362, Rm30364) and *lpdA1* mutants (Rm30396, Rm30398) were isolated. The insertional mutations in *lpdA1* and *lpdA2* of the *S. meliloti* mutants were confirmed by PCR amplification of the disrupted gene and Southern blot of the genomic DNA (Figure 5).

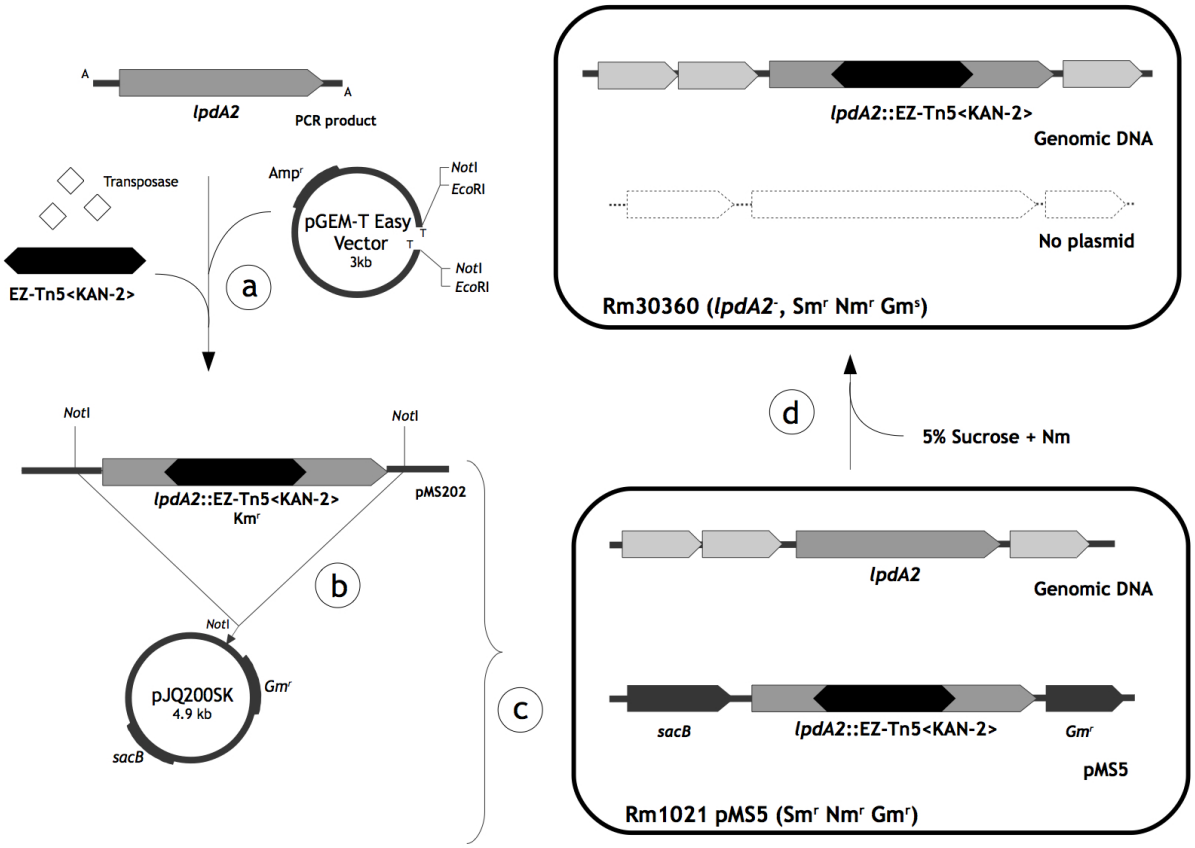

Figure 4: Construction of the *lpdA2* mutant Rm30360: an example of the procedure used for the *S. meliloti lpdA* mutants. (a) Ligation of the PCR amplified *lpdA2* gene into pGEM-T Easy (pMS2), followed by mutagenesis with EZ-Tn5<KAN-2>, resulting in pMS202. (b) Insertion of pMS202 *Not*I fragment with mutagenized *lpdA2* in *Not*I site of vector pJQ200SK. (c) Conjugation of resulting plasmid, pMS5, into Rm1021 via triparental mating. (d) Selection of double recombination events by plating conjugants on LB Nm 5% sucrose.

Figure 5: Southern blot detection of *lpdA1*ΩEZ-Tn5<TET-1> *and lpdA2*ΩEZ-Tn5<KAN-2> insertions in mutants, using DIG-labelled pMS1 (A) and pMS2 (B) as probes. Genomic DNA of each strain was restricted with *Eco*RI, including Rm30360 (lanes 4A and and 5B), Rm30362 (lanes 3A and 4B), Rm30364 (lanes 2A and 3B), Rm30366 (lanes 1A and 2B), Rm30368 (lanes 6A and 1B), and Rm1021 (lanes 7A and 6B). Lane 5A contains a partial digest of an *lpdA1* mutant. The calculated *Eco*RI restriction fragments are annotated.

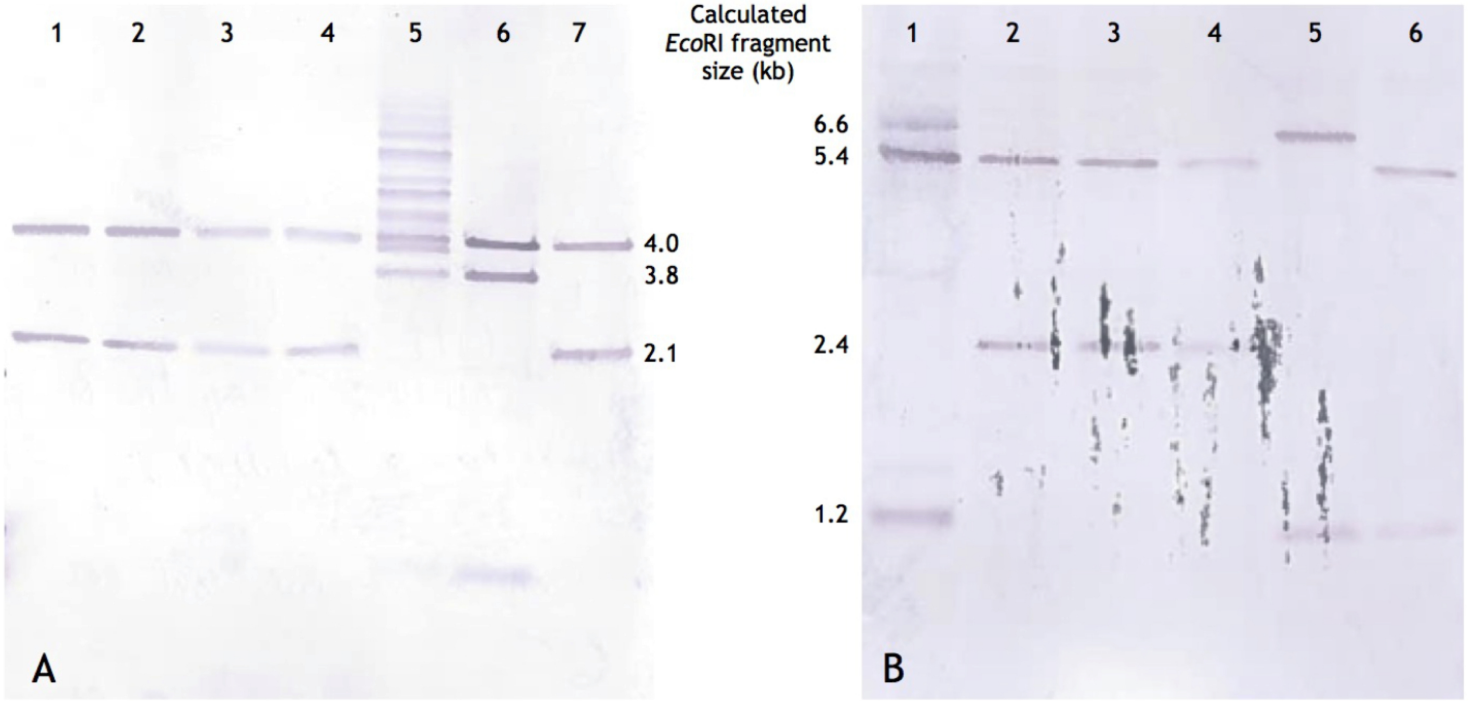
1
2
3
4
5
6
7
Calculated
*Eco*RI fragment
size (kb)
4.0
3.8
2.1
A
1
2
3
4
5
6
6.6
5.4
2.4
1.2
B

4.2 Genetic characterization of pBM1 and pBM2 complementation plasmids

The plasmids pBM1 and pBM2 were constructed by Friedman and his coworkers (1982). These plasmids consist of clone bank fragments (around 30 kb long) inside a pLAFR1 vector. The pLAFR1 vector is a 21.6 kb long low copy number plasmid that confers resistance to Tc, and which can replicate in a wide range of Gram-negative bacteria. The combination of its large plasmid size with its low copy number, resulted in difficulties to obtain high yields of plasmid DNA extracted.

A PCR analysis was performed on the plasmids pBM1 and pBM2, with primers amplifying the *lpdA1* and *lpdA2* genes. The pBM1 plasmid produced an amplicon only when the *lpdA1* primers were used, with a similar size to the *lpdA1* gene. On the other hand, the pBM2 plasmid produced an amplicon only when the *lpdA2* primers were used, with a similar size to the *lpdA2* gene. Thus, these two plasmids, containing different *lpdA* genes were good candidates for complementation analysis of the *lpdA* mutants. Analysis of their restriction pattern with *Eco*R1 also showed that pBM1 and pBM2 contain different clone bank fragments.

Only the extraction of pBM1 produced a yield high enough for sequencing the fragment. Sequencing revealed that the clone bank fragment in pBM1 is 29,929 bp long starting at *parE*780 and finishing at *ntrY*1855. Thus, this fragment of pBM1 covers the complete *pdh* operon, as well as *lpdA1*.

4.3 Growth phenotype Rm30360 (*lpdA2*) and Rm30368 (*lpdA1*)

Mutant strains Rm30360 (*lpdA2*) and Rm30368 (*lpdA1*) grew slower than wild-type

Rm1021 (Table 5). On LB plates, Rm30360 grew almost as fast as the wild type Rm1021, whereas Rm30368 took triple the amount of time to present visible colonies, even when supplementing the LB agar with carbon sources.

On the M9 plates, Rm30360 (*lpdA2*) had no growth when arabinose, pyruvate, glutamate, or β-hydroxybutyrate was the sole carbon source. Rm30360 presented a growth comparable to the wild type on plates with succinate and malate, and minimal growth was observed on glucose and α-ketoglutarate (Table 5).

When grown on liquid M9 media, Rm30360 (*lpdA2*) grew fastest on malate (Table 6), reaching stationary phase with a 6 hour delay relative to Rm1021 and with an optical density of 0.63 (95% of wild type; Figure 6B). Moreover, on the stationary phase of the malate curve, Rm30360 slowly continued its growth reaching 103% of the maximum value of Rm1021. On M9 succinate, Rm30360 grew a bit slower than with malate and reached the stationary phase with a density of 0.7 (81% of wild type), with a 12 hours delay relative to Rm1021 (Figure 6A). Growth on liquid M9 glucose followed a very similar trend to that on succinate (Figure 7B). When grown on liquid M9 arabinose, Rm30360 had a very slow growth rate and only reached an OD_{600} 19% of the wild type, not doubling the density measured right after inoculation (Figure 7A).

Rm30360 carrying plasmid pBM2 was able to grow on liquid M9 arabinose with a similar growth rate to that of wild type but reaching an OD_{600} of 0.75 (65% of wild type; Figure 7A). On glucose, succinate and malate, Rm30360 (pBM2) grew slower than Rm30360.

On the other hand, the *lpdA1* mutant Rm30368 grew only on a few carbon sources including: β-hydroxybutyric acid, arabinose and glutamate. The growth on these plates was

Table 5: Plate phenotypes of wild type *S. meliloti* 1021 and mutants Rm30368 (*lpdA1*) and Rm30360 (*lpdA2*) on M9 plates with sole carbon sources. Catabolic deficient mutants Rm30049 and Rm30277 were used as negative controls.

	Carbon source*								
Strain	gluc	pyr	α-KG	glut	ara	suc	mal	β-HB	val
Rm1021	+++	++	++	++	+++	+++	+++	++	+++
Rm30360	+	-	+	-	-	+++	+++	-	++
Rm30368	-	-	-	+	++	-	-	+	+
Rm30049	-								
Rm30277		-	-	-	-	-	-	-	

*Carbon sources: glucose (gluc), pyruvate (pyr), α-ketoglutarate (α-KG), glutamate (glut), arabinose (ara), succinate (suc), malate (mal), β-hydroxybutyrate (β-HB), and valine (val).
"+" indicates the growth intensity; "-" indicates no growth.

Table 6: Growth rates (*k*) of strains of *S. meliloti* on liquid M9 media with sole carbon sources. Strains included Rm1021 (wild type), Rm30368 (*lpdA1*), Rm30360 (*lpdA2*) and complemented mutants.

	Growth rates (*k*)			
Strain	glucose	malate	succinate	arabinose
Rm1021	0.129	0.174	0.158	0.139
Rm30360 (*lpdA2*)	0.107	0.124	0.105	0.015
Rm30368 (*lpdA1*)	0.054	0.020	0.011	0.082
Rm30360 (pBM2)	0.097	0.083	0.077	0.110
Rm30368 (pBM1)	0.103	0.121	0.121	0.109

A

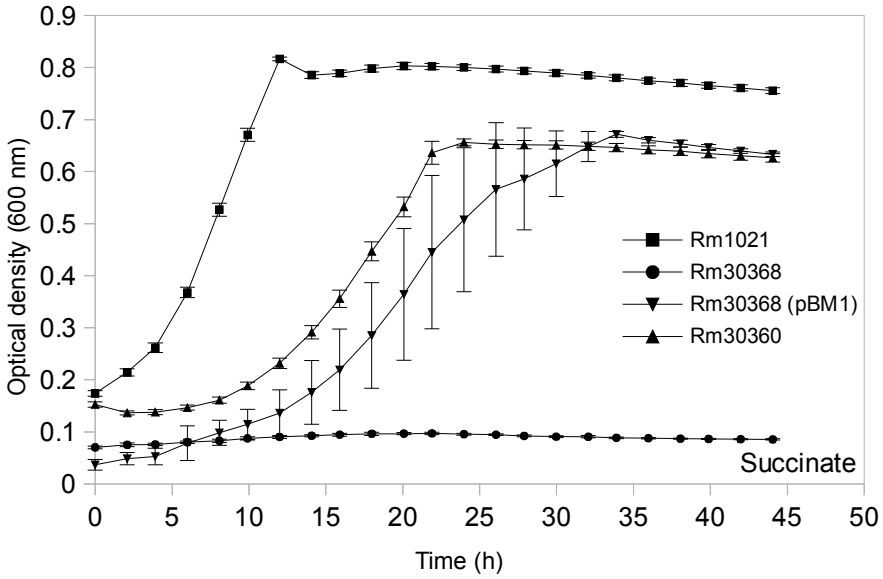

B

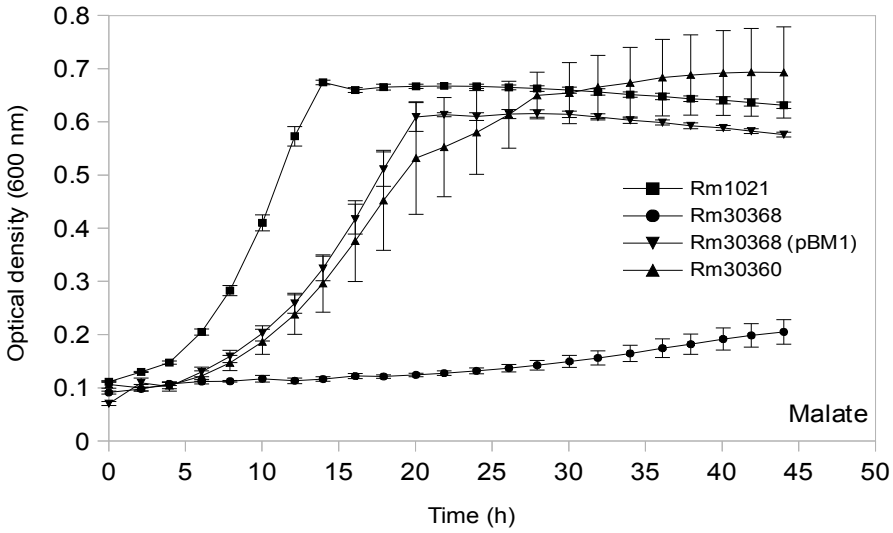

Figure 6: Growth curves of the *lpdA2* mutant Rm30360, Rm30360 carrying pBM2, the *lpdA1* mutant Rm30368, Rm30368 carrying pBM1, and wild type Rm1021 grown in M9 medium with (A) succinate and (B) malate as sole carbon sources. Values are means of optical density measurements from triplicate cultures, and the bars represent the standard errors.

A

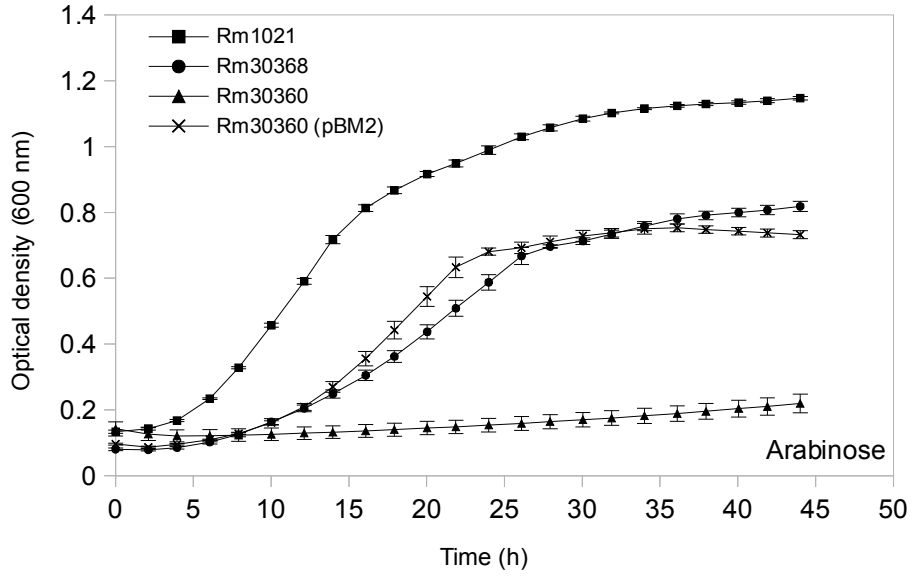

B

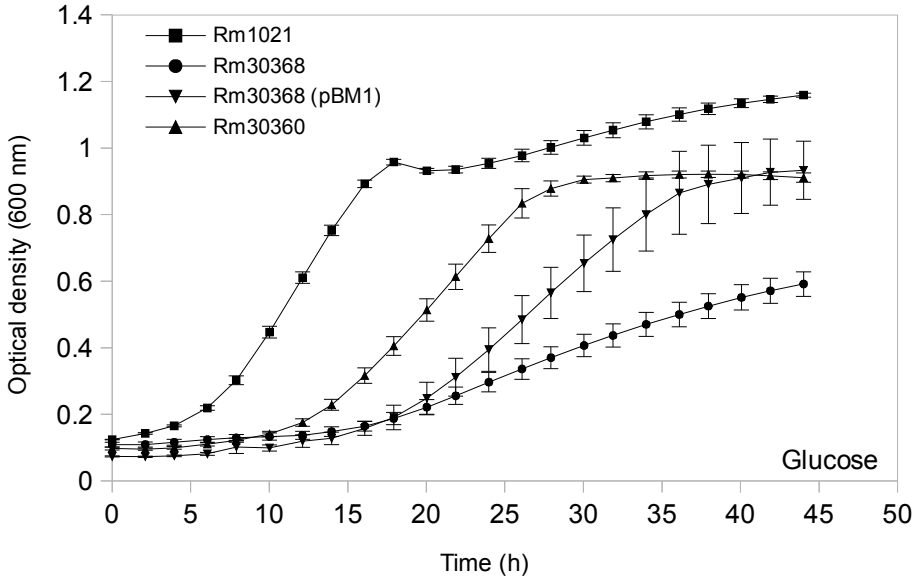

Figure 7: Growth curves of the *lpdA2* mutant Rm30360, Rm30360 carrying pBM2, the *lpdA1* mutant Rm30368, Rm30368 carrying pBM1, and wild type Rm1021 grown in M9 medium with (A) arabinose, and (B) glucose as sole carbon sources. Values are means of optical density measurements from triplicate cultures, and the bars represent the standard errors.

slower but with colonization rates almost as high as wild type Rm1021 (Table 5).

When grown on liquid minimal media, Rm30368 presented no log phase when malate (Figure 6B) or succinate (Figure 6A) were the sole carbon sources, reaching optical similar optical densities (~30%) relative to wild type. Growth on M9 arabinose was the fastest (Table 6), reaching an optical density of 0.8 (71% of wild type) with a 6 hour delay relative to wild type (Figure 7A). On M9 glucose, the growth rate was less than half the presented by wild type, reaching a final density of 51% of the maximum shown by wild type (Figure 7B).

Growth rates of Rm30368 carrying pBM1 were close to wild type levels on when grown on glucose, malate and succinate as sole carbon sources, with values two, six and eleven times higher than those of Rm30368, respectively (Table 6). On arabinose, Rm30368 (pBM1) grew 33% faster than Rm30368 (Table 6). The optical density reached by Rm30368 (pBM1) was closer to wild type levels, compared to the one reached by Rm30368, when grown on M9 glucose (Figure 7B), M9 succinate (Figure 6A) and M9 malate (Figure 6B).

4.4 Enzyme assays

The *S. meliloti lpdA1* mutant Rm30368 had no pyruvate dehydrogenase (PDH) activity (Table 7). The activity of 2-oxoglutarate dehydrogenase (OGD) was reduced to 62% of that of the wild type, and malate dehydrogenase (MDH), which was measured as a control, was 30% higher on Rm30368 than wild type.

The *S. meliloti lpdA2* mutant Rm30360 had no OGD activity (Table 8). The PDH activity was comparable to the wild type Rm1021, however the MDH activity, measured as a control, was increased 3.4-fold.

Table 7: Mean (± standard error) specific activity expressed as nmol·min^{-1}·(mg protein)$^{-1}$, of *S. meliloti lpdA1* mutant and wild type grown on M9-arabinose.

Strain	Malate dehydrogenase	2-oxoglutarate dehydrogenase	Pyruvate dehydrogenase
Rm1021	666.0 ± 11.1	32.2 ± 2.7	14.7 ± 1.0
Rm30368	838.3 ± 27.1	20.0 ± 1.0	0 ± 0

Table 8: Mean (± standard error) specific activity expressed as nmol·min^{-1}·(mg protein)$^{-1}$, of *S. meliloti lpdA2* mutant and wild type grown on M9-succinate.

Strain	Malate dehydrogenase	2-oxoglutarate dehydrogenase	Pyruvate dehydrogenase
Rm1021	512.9 ± 8.3	28.9 ± 0.6	8.2 ± 0.3
Rm30360	1733.7 ± 170.2	0.4 ± 0.4	11.2 ± 0.4

4.5 Plant growth evaluation

The alfalfa seedlings inoculated with Rm30368 and Rm30360 presented similar properties as the uninoculated control seedlings (Figures 8 and 9, Table 9). These plants were chlorotic and stunted, presenting thin roots with white pseudo-nodules attached to them. In contrast, the plants inoculated with Rm30368 carrying pBM1 and Rm30360 carrying pBM2 were green and had thick roots with pink nodules, confirming nitrogen fixation events (Figures 8 and 9). The percentage of N content and the C:N supported the observation from the dry weight analysis. Nitrogen-fixing plants had lower C:N ratios than plants that did not fix nitrogen.

Table 9: Weight, nitrogen (N) and carbon (C) content of the alfalfa plants inoculated with *S. meliloti* strains, 28 days after inoculation.

Strain	SDW[a]	%WT[b]	N content (%)[c]	C content (%)[c]	C:N	Plant phenotype
Rm1021 (*lac*)	19 ± 1	100	1.61 ± 0.04	40.4 ± 0.3	25.1	Nod^+/Fix^+
Uninoculated	7 ± 1	37	1.21 ± 0.07	38.3 ± 0.2	31.8	Nod^-/Fix^-
Rm30360 (*lpdA2*)	6 ± 0	32	1.02 ± 0.07	38.3 ± 0.5	38.6	Nod^+/Fix^-
Rm30368 (*lpdA1*)	6 ± 0	31	1.11 ± 0.03	37.5 ± 0.6	34.1	Nod^+/Fix^-
Rm30360 (pBM2)	17 ± 3	93	1.54 ± 0.08	40.3 ± 0.2	26.5	Nod^+/Fix^+
Rm30368 (pBM1)	15 ± 2	82	1.50 ± 0.02	40.8 ± 0.1	27.2	Nod^+/Fix^+

a = Shoot dry weight per plant expressed in mg ± standard error of triplicate samples (pots with 8-12 plants)
b = Percentage of the Wild Type (Rm1021) weight value.
c = Percentage of N and C content expressed as mean percentage of dry matter ± standard error of shoot DW samples used for the weight values.
Nod = nodulation
Fix = nitrogen fixation

Figure 8: Leonard's jar assembly with alfalfa plants, starting from the left, inoculated with Rm1021, Rm30360 (pBM2), Rm30360, and last an uninoculated control.

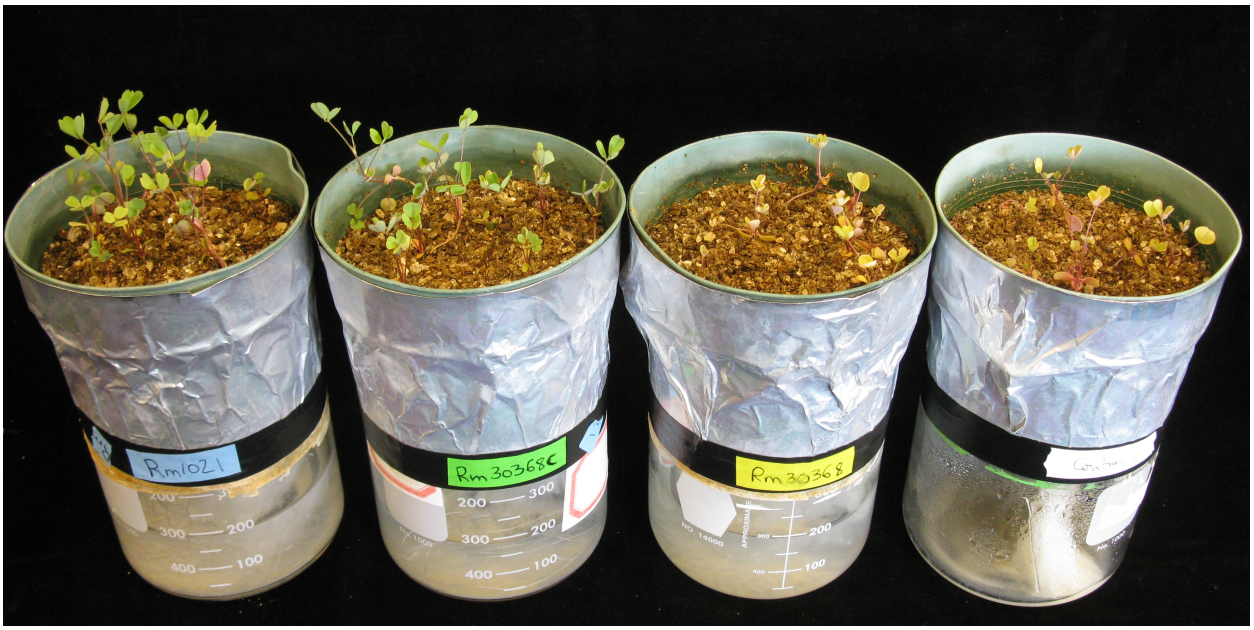

Figure 9: Leonard's jar assembly with alfalfa plants, starting from the left, inoculated with Rm1021, Rm30368 (pBM1), Rm30368, and last an uninoculated control.

5 Discussion

There are three variants of the *lpdA* gene in *S. meliloti*, and the results did not support the hypothesis that the *lpdA* gene products are interchangeable between the different complexes that contain this subunit. Results suggest that the *lpdA1* gene product is associated to the PDH complex and can not replace the function of *lpdA2* at native levels of expression. The mutation in *lpdA1* eliminated the PDH activity (Table 7). The repercussions of the decrease of acetyl-CoA, a central molecule for cellular biosynthesis and energy production, in Rm30368 (*lpdA1*) were as expected: a very deficient growth on almost all media (Table 5). The *S. meliloti lpdA1* mutant did not grow on solid minimal media with glucose as the sole carbon source, similarly to PDH mutants of other species: *B. subtilis* (Gao et al., 2006) and *R. leguminosarum* (Glenn et al., 1984). Glucose sustained a minimal growth of the *lpdA1* mutant in the liquid media (Figure 7B), likely due to energy obtained by the catabolism of glucose to pyruvate by the Entner-Doudoroff pathway (Geddes and Oresnik, 2014).

Failure of the *S. meliloti lpdA1* mutant to grow on malate or succinate on solid media (Table 5), similarly to a *P. aerugunosa* PDH mutant (Jeyaseelan and Guest, 1980), can be explained partially by the interruption of the anaplerotic reaction in which acetyl-CoA is formed from malate by the sequential activities of the malic enzyme and the PDH complex. This also leads to the lack of TCA cycle intermediates. For instance, 2-oxoglutarate is crucial for its involvement in the synthesis of glutamate and other amino acids, as demonstrated by an *S. meliloti* isocitrate dehydrogenase mutant, a glutamate auxotroph even when grown on glucose and with an intact PDH complex (McDermott and Kahn, 1992).

As expected, the *S. meliloti lpdA1* mutant grew when acetate or hydroxybutyrate was the

sole carbon source (Table 5). These carbon sources get degraded directly into acetyl-CoA with the involvement of acetyl-CoA synthetase and acetoacetyl-CoA synthetase but not the PDH complex (Cai et al., 2000). The *S. meliloti lpdA1* mutant also grew with arabinose as a sole carbon source (Table 5, Figure 7A). Arabinose is catabolized to the TCA intermediate 2-oxoglutarate in fast-growing rhizobia, such as *S. meliloti* (Duncan and Fraenkel, 1979). The cell, deficient in PDH, could be producing acetyl-CoA through lysine metabolism, which yields acetyl-CoA. Genes responsible for lysine biosynthesis using aspartate have been identified by homology in *S. meliloti* (Kyoto Encyclopedia of Genes and Genomes (KEGG) (Ogata et al. 1999)). In *S. meliloti*, aspartate aminotransferase (*aatA*) produces aspartate from oxalacetate and 2-oxoglutarate (Lodwig and Poole, 2010), two compounds hypothetically present when *S. meliloti* is grown on arabinose.

One possible occurrence of interchangeability between *lpdA*s is that of *lpdA2* by *lpdA1*. In the *S. meliloti lpdA1* mutant, there was no PDH activity, but there was 38% less OGD activity than in wild type cells (Table 7). Compared to the PDH complex, the OGD complex could be associated with the LPD encoded by *lpdA1* to a lesser extent. However, the lower activity of OGD could also be a side effect of the different metabolism in PDH mutants. Further examination of this possibility would include the phenotypic analysis of an *S. meliloti* PDH mutant with a wild type *lpdA1*. To clarify the possible interaction between the *lpdA1* product and the E1 and E2 subunits of the OGD complex, it would be necessary to create a system to overexpress *lpdA1* in the *lpdA2* mutant. In a *lpd* mutant of *P. putida*, overexpression of *lpd3*, a gene for an LPD not yet known to be specific for any complex, partially recovered the OGD complex and PDH complex activities (Palmer et al., 1991).

With the analysis of the *S. meliloti lpdA2* mutant it could be proven that the native

expression of *lpdA1* can not replace the function of the *lpdA2* (Table 8). The phenotypic properties presented by this mutant corresponded with a previous *S. meliloti* OGD mutant (Duncan and Fraenkel, 1978). The knock-out of OGD activity showed an inability to use arabinose (catabolized into 2-oxoglutarate) as a sole carbon source (Figure 7A). The *lpdA2* mutation did not interfere with the metabolism of malate, succinate, and glucose (Table 5, Figures 6 and 7B). Malate and succinate enter directly as TCA cycle intermediates, and glucose is converted to pyruvate. The anaplerotic reaction, composed of the malic enzyme and the PDH complex (unaffected by the *lpdA2* mutation), is crucial in this situation to supply acetyl-CoA and malate. These substrates can be then metabolized by the TCA cycle enzymes to produce the other TCA intermediates, necessary for other metabolic pathways.

The enzyme assays of the *S. meliloti lpdA2* mutant did not support that the *lpdA2* product is interchangeable with the *lpdA1* product in the PDH complex. The presence of wild type levels of PDH activity in the *lpdA2* mutant (Table 8) suggest *lpdA2* is likely only associated with the OGD complex. The high levels of *mdh* activity presented by this mutant in this thesis (Table 8) were not surprising. *S. meliloti* and *R. leguminosarum* strains, with mutations in the *suc* genes of the *mdh-sucCDAB* operon, presented similar polar effects on the *mdh* expression. Both *sucB* (M.Sc. Thesis, O. Trottier, 2008) and *sucD* (unpublished data) *S. meliloti* mutants, as well as *sucA* and *sucD* mutants of *R. leguminosarum* (Walshaw et al., 1997), presented an *mdh* activity at least 3 times greater than that of the wild type. The mutation of the *mdh* gene in *S. meliloti* resulted in the knock out of the *mdh* activity as well as a lower activity of all the enzymes downstream in the operon (Dymov et al., 2004).

A transcriptional regulator or promoter sequence upstream of *lpdA1* and *lpdA2* would allow independent expression in order to supply LPD subunits to different complexes. The *lpdA1*

and *lpdA2* genes, unlike the *lpdA3* gene, are not in the same operon as the genes encoding for other subunits of the complex. Mutation in *S. meliloti* by gene fusion on the gene directly upstream from *lpdA2*, *SMc02486*, a hypothetical short chain dehydrogenase/reductase, was found to have important polar effects (Jacob et al., 2008). The resulting mutant had a growth deficiency in most carbon sources, including arabinose and glutamate. We could thus assume these genes are in the same operon, and that a promoter site would be upstream of *SMc02484*, if not the same as that of the OGD operon.

The *lpdA3* gene is in the branched chain α-keto acid dehydrogenase (BKD) operon, directly downstream of the *bkdB* gene. Expression of this operon in *P. putida* is induced by the presence of branched chain aminoacids: valine, isoleucine and leucine (Massey et al., 1976). As *lpdA3* is not expressed in the conditions we used to analyze the PDH and OGD activities in this thesis, it was assumed that *lpdA3* could not interchange with *lpdA1* and *lpdA2* genes. In further studies, the carbon sources assayed should be coupled with a branched-chain amino acid to elucidate whether the *lpdA3* gene can replace the function of *lpdA1*, *lpdA2*, or both.

The *lpdA1* and *lpdA2* mutants, isolated by the use of the Tn5 transposon derivatives, proved to have stable phenotypes in media with and without antibiotic pressure, and thus were suitable for the plant growth assays, where the use of antibiotics is impractical. The plants inoculated with these mutants were chlorotic and stunted (Figure 4 and 5), suggesting a lack of nitrogen fixation, as observed in other rhizobia strains with mutations from the TCA cycle enzymes (Dymov et al., 2004; Mortimer et al., 1999; Walshaw et al., 1997; McDermott and Kahn, 1992; Gardiol et al., 1982). Thus, these results reinforce the importance of an intact TCA cycle for the energy production of the nitrogen-fixing bacteroid.

In this study, a stable *S. meliloti lpdA3* mutant could not be isolated using the EZ-

Tn5<DHFR-1> transposon. The selectable marker of this transposon encodes for a dyhidrofolate reductase, which would provide resistance to an organism against the bacteriostatic trimethoprim (Tmp), a synthetic inhibitor of folic acid metabolism. Previous studies have used this selectable marker in an *S. meliloti* host: Mueller and González (2011) using doses of up to 500 µg Tmp/ml, on unspecified media, and Trottier (2008) using doses of 350 µg Tmp/ml, on minimal media (M9 succinate). In this study, however, doses up to 700 µg Tmp/ml on minimal media (M9 succinate) did not effectively eliminate the wild type *S. meliloti* background recipient cells. Since minimal media does not contain folic acid, these results suggest that wild type *S. meliloti* possesses a metabolic pathway that bypasses the Tmp action. Efforts to isolate an *S. meliloti lpdA3* mutant should use transposons with better selectable markers in *S. meliloti*; transposon Tn5-233, which carries resistance to antibiotics gentamycin and spectinomycin, could proof itself useful for this goal (De Vos et al., 1986).

A previously isolated *S. meliloti lpdA3* mutant grew poorly on leucine and had no detectable BKD activity, confirming the association of this complex to the *lpdA3* gene (M.Sc. Thesis, B. Babic, 2010). Moreover, this implies that *lpdA1* and *lpdA2* native expression can not replace the function of *lpdA3* in the BKD complex. Repercussions on the symbiotic relationship and nitrogen fixation could not be analysed on this *lpdA3* mutant due to the instability of the *lacZ* fusion in the antibiotic-free environment. Amino acid transporters encoded by *bra* and *aap* were necessary in *R. leguminasarium* for a successful symbiosis with pea, *Pisum sativum* (Lodwig et al., 2003), since bacteroids become auxotrophs for leucine, valine and isoleucine (Prell et al., 2009). Thus, the effects of an *lpdA3* mutation in *S. meliloti* bacteroids, with the consequent knock out of BKD, could potentially be critical for the development and regulation of the bacteroid.

6 Conclusions

The results of this study suggest that *lpdA1* and *lpdA2* genes of *S. meliloti*, unlike *E. coli*, encode for LPDs associated with the PDH and OGD multi-enzyme complexes, respectively. The knock out of *lpdA1* in *S. meliloti* resulted in the lack of PDH activity and poor growth on almost all media as well as the inability to use succinate as the sole carbon source. On the other hand, the knock out of *lpdA2* in *S. meliloti* resulted in the lack of OGD activity and the inability to use arabinose as the sole carbon source. Moreover, the alfalfa plants inoculated with these mutant strains were chlorotic and stunted, showing the necessity of *lpdA1* and *lpdA2* in *S. meliloti* for a completely functional TCA cycle during symbiotic N fixation.

Findings of this study contribute to the development of *S. meliloti* as a model organism for the study of the functional characterization of the carbon catabolism genes in rhizobia. Future experiments should clarify the contribution of *lpdA1* to the OGD activity. This could be confirmed by the study of a PDH deficient strain with normal expression of *lpdA1*, or by creating a system to over-express *lpdA1* in the *S. meliloti lpdA2* mutant. The study of the gene expression and regulation of the *lpdA*s would also help with the understanding of the multiple *lpd* gene occurrence in *S. meliloti* and other organisms.

The role of *lpdA3* and BKD in *S. meliloti* should also be further studied. The function of *lpdA3* would be clarified by testing the functional replacement of *lpdA1* and *lpdA2* by the *lpdA3* gene, and by studying the repercussions of the knock out of BKD in the symbiotic relationship with alfalfa. Using the transposon EZ-Tn5<DHFR-1> needs optimization at the selection level. The isolation of a stable *S. meliloti lpdA3* mutant would also help make double and triple mutant strains that would contribute valuable information about the roles of the *lpdA* genes in *S. meliloti*.

7 References

Ambrose, M.C. and Perham, R.N. 1976. Spin-label study of the mobility of enzyme-bound lipoic acid in the pyruvate dehydrogenase multienzyme complex of *Escherichia coli*. The Biochemical Journal 155:429-432.

Babic, B. 2010. Genetic and biochemical characterization of dihydrolipoamide dehydrogenases (LPD) in *Sinorhizobium meliloti* [MSc thesis]. McGill University, Montréal, QC.

Brown, T. 2001. Southern blotting. Current protocols in inmunology Unit 10.6A: 1-13.

Cabanes, D., Boistard, P., and Batut, J. 2000. Symbiotic induction of pyruvate dehydrogenase genes from *Sinorhizobium meliloti*. Molecular plant-microbe interactions 13:483-493.

Cai, G.Q., Driscoll, B.T., and Charles, T.C. 2000. Requirement for the enzymes acetoacetyl coenzyme A synthetase and poly-3-hydroxybutyrate (PHB) synthase for growth of Sinorhizobium meliloti on PHB cycle intermediates. Journal of Bacteriology 182:2113-2118.

Capela, D., Barloy-Hubler, F., Gouzy, J., Bothe, G., Ampe, F., Batut, J., Boistard, P., Becker, A., Boutry, M., Cadieu, E., Dreano, S., Gloux, S., Godrie, T., Goffeau, A., Kahn, D., Kiss, E., Lelaure, V., Masuy, D., Pohl, T., Portetelle, D., Puhler, A., Purnelle, B., Ramsperger, U., Renard, C., Thebault, P., Vandenbol, M., Weidner, S., and Galibert, F. 2001. Analysis of the chromosome sequence of the legume symbiont *Sinorhizobium meliloti* strain 1021. Proceedings of the National Academy of Sciences of the United States of America 98: 9877-9882.

Casadesus, J. and Olivares, J. 1979. General transduction in *Rhizobium meliloti* by a thermosensitive mutant of bacteriophage DF2. Journal of Bacteriology 139: 316-317.

Chung, K. T.; Ferris, D. H. (1996). "Martinus Willem Beijerinck (1851–1931): Pioneer of General Microbiology". ASM News (Washington, D.C.: American Society For Microbiology) 62: 539-543.

Creaghan, I.T., and Guest, J.R. 1977. Suppression of the succinate requirement of lipoamide dehydrogenase mutants of *Escherichia coli* by mutations affecting succinate dehydrogenase activity. Journal of General Microbiology 102: 183-194.

de Kok, A., Hengeveld, A.F., Martin, A., and Westphal, A.H. 1998. The pyruvate dehydrogenase multi-enzyme complex from Gram-negative bacteria. Biochimica et biophysica acta 1385: 353-366.

de Vos, G.F., Walker, G.C., and Signer, E.R. 1986. Genetic manipulations in Rhizobium meliloti utilizing two new transposon Tn5 derivatives. Molecular and General Genetics 204: 485-491.

Duncan, M.J. and Fraenkel, D.G. 1979. alpha-Ketoglutarate dehydrogenase mutant of *Rhizobium meliloti*. Journal of Bacteriology 137: 415-419.

Dunn, M.F. 1998. Tricarboxylic acid cycle and anaplerotic enzymes in rhizobia. FEMS microbiology reviews 22: 105-123.

Dunn, M.F. 2014. Key roles of microsymbiont amino acid metabolism in rhizobia-legume interactions. Critical reviews in microbiology, Early Online: 1-41.

Dymov, S.l., Meek, D.J.J., Steven, B., and Driscoll, B.T. 2004. Insertion of transposon Tn 5 tac1 in the *Sinorhizobium meliloti* malate dehydrogenase (mdh) gene results in conditional polar effects on downstream TCA cycle genes. Molecular Plant-Microbe Interactions 17: 1318-1327.

Englard, S. and Siegel, L. 1969. Mitochondrial L-malate dehydrogenase of beef heart. Methods in Enzymology 13: 99-106.

Finan, T.M., Hartweig, E., LeMieux, K., Bergman, K., Walker, G.C., and Signer, E.R. 1984. General transduction in *Rhizobium meliloti*. Journal of Bacteriology 159: 120-124.

Finan, T.M., Kunkel, B., De Vos, G.F., and Signer, E.R. 1986. Second symbiotic megaplasmid in

Rhizobium meliloti carrying exopolysaccharide and thiamine synthesis genes. Journal of Bacteriology 167: 66-72.

Friedman, A.M., Long, S.R., Brown, S.E., Buikema, W.J., and Ausubel, F.M. 1982. Construction of a broad host range cosmid cloning vector and its use in the genetic analysis of Rhizobium mutants. Gene 18: 289-296.

Galibert, F., Finan, T.M., Long, S.R., Puhler, A., Abola, P., Ampe, F., Barloy-Hubler, F., Barnett, M.J., Becker, A., Boistard, P., Bothe, G., Boutry, M., Bowser, L., Buhrmester, J., Cadieu, E., Capela, D., Chain, P., Cowie, A., Davis, R.W., Dreano, S., Federspiel, N.A., Fisher, R.F., Gloux, S., Godrie, T., Goffeau, A., Golding, B., Gouzy, J., Gurjal, M., Hernandez-Lucas, I., Hong, A., Huizar, L., Hyman, R.W., Jones, T., Kahn, D., Kahn, M.L., Kalman, S., Keating, D.H., Kiss, E., Komp, C., Lalaure, V., Masuy, D., Palm, C., Peck, M.C., Pohl, T.M., Portetelle, D., Purnelle, B., Ramsperger, U., Surzycki, R., Thebault, P., Vandenbol, M., Vorholter, F.J., Weidner, S., Wells, D.H., Wong, K., Yeh, K.C., and Batut, J. 2001. The composite genome of the legume symbiont *Sinorhizobium meliloti*. Science 293:668-672.

Gao, H., Jiang, X., Pogliano, K., and Aronson, A.I. 2002. The E1beta and E2 subunits of the *Bacillus subtilis* pyruvate dehydrogenase complex are involved in regulation of sporulation. Journal of Bacteriology 184: 2780-2788.

Gardiol, A., Arias, A., Cervenansky, C., and Martinez-Drets, G. 1982. Succinate dehydrogenase mutant of *Rhizobium meliloti*. Journal of Bacteriology 151: 1621-1623.

Geddes, B.A. and Oresnik, I.J. 2014. Physiology, genetics, and biochemistry of carbon metabolism in the alphaproteobacterium *Sinorhizobium meliloti*. Canadian Journal of Microbiology 60: 491-507.

Glenn, A.R., Mckay, I.A., Arwas, R., and Dilworth, M.J. 1984. Sugar metabolism and the symbiotic properties of carbohydrate mutants of *Rhizobium-Leguminosarum*. Journal of General Microbiology 130: 239-245.

Green, L.S. and Emerich, D.W. 1997. *Bradyrhizobium japonicum* does not require alpha-ketoglutarate dehydrogenase for growth on succinate or malate. Journal of Bacteriology 179: 194-201.

Hanahan, D. 1983. Studies on transformation of *Escherichia coli* with plasmids. Journal of Molecular Biology 166: 557-580.

Hein, S. and Steinbuchel, A. 1996. Cloning and characterization of the *Alcaligenes eutrophus* 2-oxoglutarate dehydrogenase complex. FEMS Microbiology Letters 136: 231-238.

Holmes, D.S. and Quigley, M. 1981. A rapid boiling method for the preparation of bacterial plasmids. Analytical Biochemistry 114: 193-197.

Jacob, A.I., Adham, S.A.I., Capstick, D.S., Clark, S.R.D., Spence, T., and Charles, T.C. 2008. Mutational analysis of the *Sinorhizobium meliloti* short-chain dehydrogenase/reductase contribution to symbiosis family reveals substantial and catabolic diversity. Molecular Plant-Microbe Interactions 21: 979-987.

Jensen, H.L. 1942. Nitrogen fixation in leguminous plants. II. Is symbiotic nitrogen fixation influenced by *Azotobacter*? Proceedings of The Linnean Society of New South Wales 67: 205-212.

Krol, E. and Becker, A. 2004. Global transcriptional analysis of the phosphate starvation response in Sinorhizobium meliloti strains 1021 and 2011. Molecular Genetics and Genomics 272:1-17.

Leonard, L.T. 1943. A simple assembly for use in the testing of cultures of Rhizobia. Journal of Bacteriology 45: 523-527.

Li, X. and Brummer, E.C. 2012. Applied Genetics and Genomics in Alfalfa Breeding. Agronomy 2: 40-61.

Lodwig, E. and Poole, P. 2003. Metabolism of *Rhizobium* bacteroids. Critical Reviews in Plant

Sciences 22: 37-78.

Lowe, P.N., Hodgson, J.A., and Perham, R.N. 1983. Dual role of a single multienzyme complex in the oxidative decarboxylation of pyruvate and branched-chain 2-oxo acids in *Bacillus subtilis*. Biochemical Journal 215: 133-140.

Marshall, V.D., and Sokatch, J.R. 1972. Regulation of valine catabolism in *Pseudomonas putida*. J Bacteriol 110:1073-1081.

Massey, L.K., Sokatch, J.R., and Conrad, R.S. 1976. Branched-chain amino-acid catabolism in bacteria. Bacteriological Reviews 40:42-54.

Meade, H.M., Long, S.R., Ruvkin, G.B., Brown, S.E. & Ausubel, F.M.R. 1982. Physical and genetic characterization of symbiotic and auxotrophic mutants of *Rhizobium meliloti* induced by transposon Tn5 mutagenesis. Journal of Bacteriology 149: 114-122.

Ogata, H., Goto, S., Sato, K., Fujibuchi, W., Bono, H., and Kanehisa, M. 1999. KEGG: Kyoto Encyclopedia of Genes and Genomes. Nucleic acids research 27:29-34.

Paau, A.S. 1991. Improvement of *Rhizobium* inoculants by mutation, genetic engineering and formulation. Biotechnology Advances 9:173-184.

Palmer, J.A., Hatter, K., and Sokatch, J.R. 1991. Cloning and sequence-analysis of the LPD-glc structural gene of *Pseudomonas-Putida*. Journal of Bacteriology 173:3109-3116.

Palmer, J.A., Madhusudhan, K.T., Hatter, K., and Sokatch, J.R. 1991. Cloning, sequence and transcriptional analysis of the structural gene for LPD-3, the third lipoamide dehydrogenase of *Pseudomonas putida*. European Journal of Biochemistry 202: 231-240.

Payne, K.A.P., Hough, D.W., and Danson, M.J. 2010. Discovery of a putative acetoin dehydrogenase complex in the hyperthermophilic archaeon *Sulfolobus solfataricus*. FEBS Letters 584:1231-1234.

Pedrosa, F.O. and Zancan, G.T. 1974. L-Arabinose metabolism in *Rhizobium japonicum*. Journal

of Bacteriology 119: 336-338.

Peters, N.K., Frost, J.W., and Long, S.R. 1986. A plant flavone, luteolin, induces expression of Rhizobium meliloti nodulation genes. Science 233:977-980.

Prell, J., White, J.P., Bourdes, A., Bunnewell, S., Bongaerts, R.J., and Poole, P.S. 2009. Legumes regulate *Rhizobium* bacteroid development and persistence by the supply of branched-chain amino acids. Proceedings of the National Academy of Sciences of the United States of America 106: 12477-12482.

Quail, M.A., Haydon, D.J., and Guest, J.R. 1994. The pdhR-aceEF-lpd operon of *Escherichia coli* expresses the pyruvate dehydrogenase complex. Molecular Microbiology 12: 95-104.

Quandt, J. and Hynes, M.F. 1993. Versatile suicide vectors which allow direct selection for gene replacement in gram-negative bacteria. Gene 127:15-21.

Reed, L.J. and Mukherjee, B.B. 1969. α-ketoglutarate dehydrogenase complex from *Escherichia coli*. Methods in Enzymology 13: 55-61

Sadowsky, M.J., Keyser, H.H., and Benbohlool, B. 1983. Biochemical-characterization of fast-growing and slow-growing Rhizobia that nodulate soybeans. International Journal of Systematic Bacteriology 33:716-722.

Sambrook, J.R.D.W. 2001. Molecular cloning: a laboratory manual. Cold Spring Harbor Laboratory Press, Cold Spring Harbor, N.Y.

Sanger, F., Nicklen, S., and Coulson, A.R. 1977. DNA sequencing with chain-terminating inhibitors. Proceedings of the National Academy of Sciences of the United States of America 74:5463-5467.

Schwinde, J.W., Hertz, P.F., Sahm, H., Eikmanns, B.J., and Guyonvarch, A. 2001. Lipoamide dehydrogenase from Corynebacterium glutamicum: molecular and physiological analysis of the lpd gene and characterization of the enzyme. Microbiol-Sgm 147:2223-2231.

Sokatch, J.R., Mccully, V., Gebrosky, J., and Sokatch, D.J. 1981. Isolation of a specific lipoamide dehydrogenase for a branched-chain keto acid dehydrogenase from *Pseudomonas putida*. Journal of Bacteriology 148:639-646.

Soto, M.J., Sanjuan, J., and Olivares, J. 2001. The disruption of a gene encoding a putative arylesterase impairs pyruvate dehydrogenase complex activity and nitrogen fixation in Sinorhizobium meliloti. Molecular Plant-Microbe Interactions 14:811-815.

Steiert, P.S., Stauffer, L.T., and Stauffer, G.V. 1990. The Lpd gene-product functions as the L protein in the *Escherichia coli* glycine cleavage enzyme-system. Journal of Bacteriology 172:6142-6144.

Sulieman, S., Schulze, J., and Tran, L.S. 2013. Comparative analysis of the symbiotic efficiency of *Medicago truncatula* and *Medicago sativa* under phosphorus deficiency. International Journal of Molecular Sciences 14:5198-5213.

Trottier, O. 2008. Genetic Characterization of gamma-aminobutyrate metabolism in *Sinorhizobium meliloti* [MSc thesis]. McGill University, Montréal, QC.

Udvardi, M., and Poole, P.S. 2013. Transport and metabolism in legume-rhizobia symbioses. Annual Review of Plant Biology 64:781-805.

Walshaw, D.L., Wilkinson, A., Mundy, M., Smith, M., and Poole, P.S. 1997. Regulation of the TCA cycle and the general amino acid permease by overflow metabolism in *Rhizobium leguminosarum*. Microbiology 143: 2209-2221.